INVESTIGATION OF BREVETOXIN INTERACTIONS WITH EXCITABLE MEMBRANES OF THE MARINE DIATOM *ODONTELLA SINENSIS*

Sheila Ann Kitchen

A Thesis Submitted to the
University of North Carolina Wilmington in Partial Fulfillment
of the Requirements for the Degree of
Master of Science

Department of Biology and Marine Biology

University of North Carolina Wilmington

2010

Approved by

Advisory Committee

Andrea Bourdelais

J. Craig Bailey

Carmelo Tomas

Alison Taylor
Chair

Accepted by

DN: cn=Robert D. Roer, o=UNCW, ou=Dean of the Graduate School & Research, email=roer@uncw.edu, c=US
Date: 2010.10.28 10:57:55 -04'00'

Dean, Graduate School

TABLE OF CONTENTS

ACKNOWLEDGEMENTS v

LIST OF TABLES vi

LIST OF FIGURES vii

CHAPTER ONE: LITERATURE REVIEW OF THE DINOFLAGELLATE *KARENIA BREVIS* AND ITS TOXINS 1

Ecology of *K. brevis* and HABs 2

Allelopathy and HABs 5

Voltage Gated Sodium Channel as a Mechanism of Marine Toxin Interactions 7

Brevetoxins 8

Evolution of Marine Phytoplankton and Evidence for Membrane Excitability 10

References 12

CHAPTER TWO: MOLECULAR INVESTIGATION OF VOLTAGE-GATED ION CHANNELS IN CHROMALVEOLATES 16

Abstract 17

Introduction 17

Results 21

Discussion 23

Material and Methods 26

Table and Figures 27

References 36

CHAPTER THREE: BREVETOXIN SENSITIVE IONIC CURRENTS IN THE MARINE DIATOM *ODONTELLA SINENSIS* 40

Abstract 41

Introduction 42

Results 44

Discussion 49

Material and Methods 53

Figures 59

References 79

ACKNOWLEDGEMENTS

First and foremost I would like to express my gratitude to my graduate advisor Dr. Alison Taylor. She was a gracious guide through the throes of the Masters program at UNCW. I not only benefited from her scientific wisdom, insight and expertise in the lab but she also played an instrumental role in encouraging me to continue on with science into the next phase of my academic career. Furthermore, the laboratory techniques I acquired under Dr. Taylor's direction will be instrumental to my future research, and for that I am indebted to her.

I would also like to thank my committee members Dr. Carmelo Tomas, Dr. Andrea Bourdelais, and Dr. J. Craig Bailey for their commitment to my success over the span of the thesis project. Each member was able to provide a unique perspective in their area of expertise to my thesis objectives which greatly enhanced my final product. Additionally, I would like to thank those individuals from the UNCW microscopy lab, Dr. Baden's lab, Dr. Tomas's lab and Dr. Bailey's lab who provided technical assistance throughout my research project. Specifically I want to recognize Mark Gay, Elizabeth Elliot, Harris Muhlsteinn and Cory Dasheill for sharing their specialized knowledge of microscopy, phytoplankton culturing and molecular techniques.

Finally, I want to show my appreciation for the continued support from my friends and family. Over the course of the masters program when I began to doubt myself, their reassurance and optimism in my abilities to succeed did not go unnoticed. I cannot thank them enough for providing happy distractions when I was overwhelmed with school work or research.

LIST OF TABLES

CHAPTER TWO

Table 1. Genomic evidence of voltage-gated Na^+ or Ca^{2+} channels.....27

LIST OF FIGURES

CHAPTER TWO

Figure 1. Pore domain analysis of putative Na^+/Ca^{2+} VGCs of chromalveolates.....30

Figure 2. Inactivation gate in chromalveolates.....32

Figure 3. Phylogenetic analysis of voltage-gated Ca^{2+} and Na^+ channels in eukaryotes...34

CHAPTER THREE

Figure 1. Brevetoxin binding site on voltage-gated Na^+ channels.....59

Figure 2. Uptake and cellular localization of Bodipy-PbTx-B in *Odontella sinensis* 61

Figure 3. *K. brevis* is resistant to Bodipy-PbTx-B uptake. 63

Figure 4. Spontaneous and evoked action potentials in *O. sinensis*. 65

Figure 5. Effect of PbTx-3 on the membrane potential of *O. sinensis*. 67

Figure 6. Effect of PbTx-3 on voltage activated currents of *O. sinensis*. 69

Figure 7. Summary of lidocaine and PbTx inhibition of *O. sinensis* VGCs.....71

Figure 8. Activation kinetics of *O. sinensis* VGCs are unaffected by PbTx-3. 73

Figure 9. Inactivation kinetics of *O. sinensis* VGCs in the presence of PbTx-3 75

Figure 10. Recovery from inactivation of *O. sinensis* VGCs is unaffected by PbTx-3.....77

CHAPTER ONE

LITERATURE REVIEW OF THE DINOFLAGELLATE *KARENIA BREVIS* AND ITS TOXINS

Marine phytoplankton growth is dependent on multiple environmental factors including: temperature, salinity, irradiance, nutrient availability and competition. These factors are assumed to be specific for each algal species, and under favorable conditions "blooms" of a single planktonic species can occur [1,2]. Of the approximately 4,000 phytoplankton species known, about 300 are bloom forming including: diatoms, dinoflagellates, silicoflagellates, prymnesiophytes and raphidophytes [3]. Within the 300 taxa, 60 to 80 species are considered harmful or toxic and three quarters of which are dinoflagellates [4]. Toxic algae are generally present in low concentrations with little or no effect on the surrounding ecosystem, but when dense aggregations of cells occur under bloom conditions, the toxins become an environmental concern [5].

Recently there has been an increase in the frequency, duration and geographic distribution of algal blooms [6]. Anthropogenic activities may directly contribute to these trends in bloom initiation through eutrophication and ballast water transfer resulting in widespread and persistent blooms. These events may be exacerbated indirectly by rapid global climate change and the resultant changes in weather patterns [7].

I. *Ecology of K. brevis and HABs*

Harmful algal blooms (HABs) present a growing problem for fisheries, aquaculture, tourism and public health. HABs have direct effects on animals and humans in contact with waterborne or aerosolized toxins as well as indirect effects through consumption of contaminated prey species [4,5,8]. In the Gulf of Mexico, predominantly along the southwestern Florida coast, the most prevalent blooms are caused by the dinoflagellate *Karenia brevis* that have been documented since 1648 [9]. *K. brevis* is an athecate, small to medium-sized (18-45μm wide)

photosynthetic dinoflagellate [10]. It has four membranes surrounding the cytoplasm with microtubules found between the plasmalemma and innermost membrane around the cingulum, sulcus and flagellar canal [11]. The chloroplasts are located at the periphery of the cell (10-20 per cell) and contain chlorophyll *a* and accessory pigments fucoxanthin, β-carotene, diadinoxanthin, and gyroxanthin-diester diagnostic of *Karenia* spp. [9,11]. The nucleus is located in the left hypocone and has permanently condensed chromosomes [11,12]. The life cycle of *K. brevis* is similar to other dinoflagellates having both vegetative and sexual life stages; however a resting cyst of *K. brevis* has yet to be described. The location of brevetoxin biosynthesis and organelle or vesicle compartmentalization within the cell remains unresolved. Nevertheless, a *K. brevis* gene coding for a novel Type-1 polyketide synthase protein, thought to play a role in the production of brevetoxins, has recently been determined [13,14,15].

Along the coast of Florida, *K. brevis* blooms (10^3 to 10^7 cells L^{-1}) occur periodically resulting in detrimental effects on the local ecosystem and economy. The lack of a rigid cellulose wall of *K. brevis* cells facilitates lysis in turbulent waters, subsequently causing intracellular toxins to be dispersed into the surrounding waters [5,12]. Such bloom events result in massive fish, marine mammal, sea turtle, and sea bird mortalities in addition to causing hypoxic conditions negatively impacting sea grass and coral reef communities [6,12]. These mass mortalities can engender trophic disruptions, close fishery and decrease tourism.

Low concentrations of *K. brevis* cells are always present in offshore oligotrophic Gulf water. The cells are transported to coastal regions via the Loop Current where they are exposed to higher nutrient levels that arise from upwelling events, agricultural runoff and riverine input [9,16]. The Loop Current moves in the clockwise direction and forms the Florida current around

the Straits of Florida where it flows into the Gulf Stream. Periodically there is transport of *K. brevis* northward along the eastern coast of the United States. More commonly, eddies break off from the Loop Current to disperse cells westward toward the Gulf coast of Texas and Mexico.

In oligotrophic waters, *K. brevis* growth is relatively slow and limited by nitrogen availability [4,17,18]. However, under nutrient replete conditions, generally dinoflagellates have higher affinity for available nutrients than other phytoplankton species such as the diatoms and this may be one of the factors that allows *K. brevis* to outcompete other phytoplankton species [16,19,20]. Ryther [21] showed that *K. brevis* was able to grow equally well on both dissolved organic nitrogen sources such as urea and inorganic nitrogen sources of nitrate and ammonium. Thus, conferring an additional competitive advantage of these cells over other phytoplankton that can only use organic nitrogen sources.

K. brevis bloom initiation in offshore waters is correlated with high irradiance leading to phototactic-induced vertical migrations to surface waters, often discoloring the water in red, brown and/or yellow hues [22]. Studies have shown *K. brevis* is capable of adapting to variable irradiance and UV levels by altering chlorophyll and accessory pigment concentrations over a generation time[16]. Blooms are also correlated with low salinity events following high input of freshwater through riverine inflow, rainfall or groundwater, and eutrophication caused by terrestrial weathering, anthropogenic activities and large storm systems such as hurricanes [4,17,18]. Another hypothesis to explain *K. brevis* bloom initiation was proposed by Walsh and Steidinger [23] based on iron rich Saharan dust deposited into the Gulf of Mexico. They propose that iron influx can stimulate the growth of iron limited *Tricodesmium*, a cyanobacterium that

fixes atmospheric nitrogen gas, enriching the waters with organic nitrogen and thus initiating small blooms of nitrogen limited *K. brevis* [16].

II. *Allelopathy and HABs*

Competition is one of the primary ecological factors that govern marine community structure. It was suggested that competition among planktonic species might initiate the biosynthesis of algal toxins [24,25,26]. Allelopathy refers to a chemically mediated competition strategy by the production and release of secondary metabolites that inhibit competitors' growth and development [1,4,24,27,28]. As an example, *Prymnesium parvum,* a haptophyte found in many coastal plankton communities and known to cause severe ecological damage, caused significant reduction of cell growth and increased mortality of other phytoplankton exposed to cell-free *P. parvum* filtrate [1]. Another example of allelopathic plankton is *Alexandrium* spp. that produces a range of secondary metabolites including saxitoxin. Saxitoxin is thought to be an anti-predation metabolite against major grazers which has been confirmed in some laboratory experiments showing copepods exhibit positive selection for non-toxic prey over *Alexandrium* [29,30]. In field experiments at high concentrations of toxic *Alexandrium,* copepods exhibited reduced feeding rates resulting in lower growth rates [30]. *Alexandrium* spp. were also found to have detrimental effects on both prokaryote and eukaryote cells in response to uncharacterized extracellular lytic metabolites, unrelated to saxitoxin production, increasing *Alexandrium* competitive advantage among other plankton [28].

Whether brevetoxins are produced as an allelopathic defense mechanism remains unclear. Decreased fecundity and succession of copepods [31,32] and rotifers [33] was observed when a sole diet of *K. brevis* was provided suggesting a possible role in anti-predation. However, few

studies have addressed these toxins as a competitive allelochemical against other ecologically relevant targets such as phytoplankton. Experimental data supports negative effects on growth rates of 20 different species of phytoplankton representing four different phyla from exposure to both *K. brevis* incubated water and purified brevetoxins [2]. This work has since been expanded to include non-toxic dinoflagellates, diatoms, chlorophytes and cryptophytes typical of the coast of Florida [27], resulting in a range of both positive and negative species specific growth responses in the presence of live *K. brevis* cells, extracellular filtrates and purified toxins. Of the phytoplankton assessed, only the dinoflagellates and diatoms were negatively affected by exposure to live *K. brevis* and its extracts, whereas other species were less susceptible to brevetoxin effects [27]. Although these experiments demonstrate allelopathic effects on non-toxic phytoplankton, the degree of growth inhibition varied considerably and could not be directly attributed to brevetoxin alone. Moreover, the cellular mechanism of the observed allelopathic effects of *K. brevis* metabolites is unknown.

Interestingly, *K. brevis* growth can be negatively affected by the presence of other phytoplankton in the live cultures, suggesting that *K. brevis* may have limited resistance to its own toxins or secondary metabolites [27]. At least five phytoplankton species are able to reduce the level of brevetoxin in the surrounding water [34]. These results support the contention that co-occurring phytoplankton may have evolved one or more mechanisms for detoxifying brevetoxin.

Whether or not *K. brevis* produces allelopathic compounds that suppress cell growth in other phytoplankton remains inconclusive given the varying reports discussed above. Further

analyses are needed to assess the cellular mechanisms by which these toxic metabolites influence phytoplankton growth and reproduction and how this relates to interspecific competition.

III. *Voltage Gated Sodium Channel as a Mechanism of Marine Toxin Interactions*

As discussed above, algal toxins produced by marine organisms are thought to function in chemical defense [1,2,28,29,33,35,36]. Many of these toxins exert their effect on animals because they are highly specific inhibitors of plasma membrane ion channels resulting in major alterations of cell signaling processes. For example, the diatom *Pseudo-Nitzschia* produces domoic acid that causes amnesic shellfish poisoning by actively competing with kainite and glutamate receptors in the central nervous system thus altering neurotransmitter release [37]. Domoic acid binding results in repetitive depolarizations of the nerve cell membrane leading to elevated intracellular calcium levels, increased exocytosis of synaptic vesicles and ultimately cell death [5].

The target for many algal toxins appears to be voltage-gated sodium channels (VGSC); the transmembrane proteins responsible for voltage-dependent Na^+ influx, membrane depolarization and the initiation of action potentials in animal neuromuscular systems [38]. The animal Na^+ channel comprises four domains each containing six transmembrane segments (6TM) designated S1-S6 [26,38]. The S4 segment of each domain contains positively charged arginine residues that act as voltage sensors for channel activation [39]. Voltage dependent inactivation of Na^+ channels is controlled by a short intracellular loop connecting domains III and IV that blocks the pore during depolarization [39]. These structural motifs are well conserved, have been thoroughly characterized and can be used as features to identify Na^+ channel homologues [40,41,42].

In animals, specific isoforms of the VGSC's are particularly sensitive to marine toxins derived from algae. The algal neurotoxins, brevetoxin, saxitoxin and ciguatoxin, at pM-nM concentrations can result in neuro-muscular dysfunction in humans. Clinical symptoms include nausea, vomiting, diarrhea, and upon higher exposure to the toxins temperature sensation reversal, numbing of extremities, paralysis and death. Paralytic shellfish poisoning is caused by dinoflagellate derived saxitoxins from *Alexandrium sp.* binding to the extracellular receptor site 1 on the VGSC, blocking Na^+ based action potentials with a 0.1 to 1 mg dose being lethal to humans [38,43]. Tetrodotoxin, found in the puffer fish, also shows high affinity for site 1 on the Na^+ channel and an LD_{50} of 10µg/kg in mice [44]. Both saxitoxin and tertodotoxin have been used to resolve the receptor site 1 of the VGSC which comprises conserved amino acid residues on the S6 transmembrane segment of each protein domain [26,38]. Ciguatoxin, which causes ciguatera fish poisoning, demonstrates a high affinity for site 5 on the VGSC [45,46] causing a conformational change in VGSC to the open state, a shift in activation to more negative membrane potentials and a block of inactivation [38,47].

IV. *Brevetoxins*

K. brevis produces a suite of polycyclic ether neurotoxins called brevetoxins. Since their discovery, brevetoxins have been intensely studied to understand their pharmacology [38,45,46,47,48,49,50], biosynthesis [13,14,51,52] and biotechnological applications [8,17,53]. They have been tested on a wide variety of *in vitro* mammalian neuronal preparations [47,54] to identify toxin interaction. Brevetoxins are classified by the chemical structure of their polyether ladder backbone and derivatives are produced through intermediary metabolism and environmental decomposition [54,55]. The brevetoxins PbTx-1 and PbTx-2 are the most toxic

forms. They specifically bind to site 5 on the VGSCs, actively competing with ciguatoxins site 5 on VGSC's [5,45,54]. In animal nerve cells, brevetoxins alter voltage activation and inhibit fast channel inactivation resulting in prolonged channel opening and hyperexcitablity of the cell [12,47]. However, there have been no studies of the effects of brevetoxins on ion channels and cellular signaling processes in phytoplankton.

Brevetoxins not only interfere with neuromuscular signals but also cause a prolonged influx of calcium (Ca^{2+}) into the cell that has been shown to cause neuronal injury [47,48]. Previous experiments have quantified the influx of Ca^{2+} into cerebellar granule neurons from Sprague-Dawley rats under the influence of natural and semi-synthetic brevetoxins using the fluorescent dye Fluo 3 and found that of PbTx-1, PbTx-2 and PbTx-3, PbTx-1 caused the largest increase in intracellular Ca^{2+} [47]. It was also shown that action potential dependent intracellular Ca^{2+} oscillations in neocortical neurons were sensitive to brevetoxins [48]. Given that changes in cytoplasmic Ca^{2+} are a common mode of signaling in both excitable and non-excitable cells [48] it will be of great interest to determine whether or not the reported toxicity of brevetoxins in phytoplankton cells occurs as a result of induced elevations of cytoplasmic Ca^{2+}.

Recently, a non-toxic molecule, brevenal, was isolated from *K. brevis* cultures and shown to actively compete with brevetoxins for site 5 on the VGSC [8]. The concentration of this site 5 antagonist increases as *K. brevis* cell density increases and is present throughout the bloom [8]. The function and biosynthetic pathway of brevenal is still unresolved, but its potential as a therapeutic compound in, for example, brevetoxin-affected humans has been suggested [8]. One functional role of brevenal production by *K. brevis* could correspond to providing protection from their own brevetoxins [2,6,8,27]. Further investigation is needed to resolve the effects that

brevenal concentrations have on *K. brevis* and on the membrane physiology of other phytoplankton.

V. *Evolution of Marine Phytoplankton and Evidence for Membrane Excitability*

Evolutionary studies suggest that plastids arose once via the endosymbiosis of cyanobacteria and have subsequently been laterally transferred to the last common ancestor of the chromalveolates via secondary endosymbiosis of a red alga [12,56,57,58]. Genome analyses of the diatom *Thalassiosira pseudonana* revealed 806 proteins that aligned only with heterotrophic eukaryote proteins sequences, but not green or red algae, suggesting that these proteins were derived from the host [58]. Thus, during endosymbiotic events that gave rise to photosynthetic eukaryotes, "animal-like" nuclear genes have been conserved; included among these conserved host gene families are the voltage-gated ion channels which underlie cellular signaling.

Biophysical evidence for the presence of such voltage-gated ion channels in key phytoplankton groups includes the dinoflagellates, diatoms and coccolithophores. The dinoflagellate *Noctiluca miliaris* has shown a fast flash-triggering action potential from voltage stimulus that produces bioluminescence and feeding tentacle coiling [59,60]. Moreover, diatoms and coccolithophorids have recently been shown to possess excitable membranes that upon depolarization generate fast "animal-like" action potentials including a fast (ms) inward current followed by a rapid (s) repolarization of the membrane [61,62]. Biophysical evidence for the presence of an action potential prior to the divergence of the opisthokonts is accumulating [26,61,62]. Genome analysis also supports the contention that the evolution of the VGCs lies much deeper within the eukaryotes than has been suspected [61,62,63] and that Na^{+}/Ca^{2+} VGCs

play a much broader and evolutionary significant role in eukaryote cell signaling. These recent studies on phytoplankton cellular signaling also raise the question of whether such algal voltage activated ion channels may be ecologically relevant targets for toxins such as the brevetoxins.

References

1. Fistarol GO, Legrand C, Graneli E (2003) Allelopathic effect of *Prymnesium parvum* on a natural plankton community. Marine Ecology-Progress Series 255: 115-125.
2. Freeberg LA, Marshall A, Heyl M (1978) Interrelationships of *Gymnodinium breve* (Florida red tide) within the phytoplankton community. In: Taylor DL, Seliger HH, editors. Toxic Dinoflagellate Blooms. 1978 ed. New York: Elsevier. pp. 139-144.
3. Sournia A (1995) Red-tide and toxic marine phytoplankton of the world ocean: An inquiry into biodiversity. Harmful marine algal blooms Proceeding of 6th International Conference on Toxic Marine Phytoplankton: Lavoisier. pp. 103-112.
4. Smayda TJ (1997) Harmful algal blooms: Their ecophysiology and general relevance to phytoplankton blooms in the sea. Limnology and Oceanography 42: 1137-1153.
5. Van Dolah FM (2000) Marine algal toxins: Origins, health effects, and their increased occurrence. Environmental Health Perspectives 108: 133-141.
6. Pierce RH, Henry MS (2008) Harmful algal toxins of the Florida red tide (*Karenia brevis*): natural chemical stressors in South Florida coastal ecosystems. Ecotoxicology 17: 623-631.
7. Paerl HW, Whitall DR (1999) Anthropogenically-derived atmospheric nitrogen deposition, marine eutrophication and harmful algal bloom expansion: Is there a link? Ambio 28: 307-311.
8. Bourdelais AJ, Campbell S, Jacocks H, Naar J, Wright JLC, et al. (2004) Brevenal is a natural inhibitor of brevetoxin action in sodium channel receptor binding assays. Cellular and Molecular Neurobiology 24: 553-563.
9. Steidinger KA (2009) Historical perspective on *Karenia brevis* red tide research in the Gulf of Mexico. Harmful Algae 8: 549-561.
10. Haywood AJ, Steidinger KA, Truby EW, Bergquist PR, Bergquist PL, et al. (2004) Comparative morphology and molecular phylogenetic analysis of three new species of the genus *Karenia* (Dinophyceae) from New Zealand. Journal of Phycology 40: 165-179.
11. Steidinger KA, Truby EW, Dawes CJ (1978) Ultrastructure of the red tide dinoflagellate *Gymnodium breve*. I. General description. Journal of Phycology 14: 72-79.
12. Hackett JD, Anderson DM, Erdner DL, Bhattacharya D (2004) Dinoflagellates: A remarkable evolutionary experiment. American Journal of Botany 91: 1523-1534.
13. Snyder RV, Guerrero MA, Sinigalliano CD, Winshell J, Perez R, et al. (2005) Localization of polyketide synthase encoding genes to the toxic dinoflagellate Karenia brevis. Phytochemistry 66: 1767-1780.
14. Monroe EA, Van Dolah FM (2008) The toxic dinoflagellate *Karenia brevis* encodes novel type I-like polyketide synthases containing discrete catalytic domains. Protist 159: 471-482.
15. López-Legentil S, Song B, DeTure M, Baden D (2010) Characterization and localization of a hybrid non-ribosomal peptide synthetase and polyketide synthase gene from the toxic dinoflagellate *Karenia brevis*. Marine Biotechnology 12: 32-41.
16. Vargo GA (2009) A brief summary of the physiology and ecology of *Karenia brevis* Davis (G. Hansen and Moestrup comb. nov.) red tides on the West Florida Shelf and of hypotheses posed for their initiation, growth, maintenance, and termination. Harmful Algae 8: 573-584.

17. Richardson TL, Pinckney JL, Walker EA, Marshalonis DM (2006) Photopigment radiolabelling as a tool for determining in situ growth rates of the toxic dinoflagellate *Karenia brevis* (Dinophyceae). European Journal of Phycology 41: 415-423.
18. Yentsch CS, Lapointe BE, Poulton N, Phinney DA (2008) Anatomy of a red tide bloom off the southwest coast of Florida. Harmful Algae 7: 817-826.
19. Doucette GJ, Harrison PJ (1990) Some effects of iron and nitrogen stress on the red tide dinoflagellate *Gymnodinium sanguineum.* Marine Ecology-Progress Series 62: 293-306.
20. Aksnes DL, Egge JK (1991) A theoretical model for nutrient uptake in phytoplankton Marine Ecology-Progress Series 70: 65-72.
21. Ryther JH (1955) Ecology of autotrophic marine dinoflagellates with reference to red water conditions. In: Johnson FH, editor. The Luminescence of Biological Systems. Washington, DC: American Association of Advance Science. pp. 387-414.
22. Millie DF, Schofield OM, Kirkpatrick GJ, Johnsen G, Tester PA, et al. (1995) Relating photosynthetic pigments and in vivo optical density spectra to irradiance for the Florida red-tide dinoflagellate *Gymnodinium breve*. Marine Ecology Progress Series 120: 65-75.
23. Walsh JJ, Steidinger KA (2001) Saharan dust and Florida red tides: The cyanophyte connection. Journal of Geophysical Research Oceans 106: 11597-11612.
24. Legrand C, Rengefors K, Fistarol GO, Graneli E (2003) Allelopathy in phytoplankton - biochemical, ecological and evolutionary aspects. Phycologia 42: 406-419.
25. Hutchinson GE (1961) The Paradox of the Plankton. The American Naturalist 95: 137.
26. Anderson PAV, Roberts-Misterly J, Greenberg RM (2005) The evolution of voltage-gated sodium channels: were algal toxins involved? Harmful Algae 4: 95-107.
27. Kubanek J, Hicks MK, Naar J, Villareal TA (2005) Does the red tide dinoflagellate *Karenia brevis* use allelopathy to outcompete other phytoplankton? Limnology and Oceanography 50: 883-895.
28. Tillmann U, Alpermann T, John U, Cembella A (2008) Allelochemical interactions and short-term effects of the dinoflagellate *Alexandrium* on selected photoautotrophic and heterotrophic protists. Harmful Algae 7: 52-64.
29. Teegarden GJ (1999) Copepod grazing selection and particle discrimination on the basis of PSP toxin content. Marine Ecology-Progress Series 181: 163-176.
30. Teegarden GJ, Campbell RG, Anson DT, Ouellett A, Westman BA, et al. (2008) Copepod feeding response to varying *Alexandrium* spp. cellular toxicity and cell concentration among natural plankton samples. Harmful Algae 7: 33-44.
31. Cohen JH, Tester PA, Forward RB, Jr. (2007) Sublethal effects of the toxic dinoflagellate *Karenia brevis* on marine copepod behavior. Journal of Plankton Research 29: 301-315.
32. Breier CF, Buskey EJ (2007) Effects of the red tide dinoflagellate, *Karenia brevis*, on grazing and fecundity in the copepod *Acartia tonsa*. Journal of Plankton Research 29: 115-126.
33. Kubanek J, Snell TW, Pirkle C (2007) Chemical defense of the red tide dinoflagellate *Karenia brevis* against rotifer grazing. Limnology and Oceanography 52: 1026-1035.
34. Myers TL, Prince EK, Naar J, Kubanek J (2008) Loss of waterborne brevetoxins from exposure to phytoplankton competitors. Harmful Algae 7: 762-771.
35. Nejstgaard JC, Solberg PT (1996) Repression of copepod feeding and fecundity by the toxic haptophyte *Prymnesium patelliferum*. Sarsia 81: 339-344.

36. Miralto A, Barone G, Romano G, Poulet SA, Ianora A, et al. (1999) The insidious effect of diatoms on copepod reproduction. Nature 402: 173.
37. Hampson DR, Huang X-p, Wells JW, Walter JA, Wright JLC (1992) Interaction of domoic acid and several derivatives with kainic acid and AMPA binding sites in rat brain. European Journal of Pharmacology 218: 1-8.
38. Cestele S, Catterall WA (2000) Molecular mechanisms of neurotoxin action on voltage-gated sodium channels. Biochimie 82: 883-892.
39. Catterall WA, Goldin AL, Waxman SG (2003) International union of pharmacology. XXXIX. Compendium of voltage-gated ion channels: sodium channels. Pharmacological Reviews 55: 575-578.
40. West JW, Patton DE, Scheuer T, Wang Y, Goldin AL, et al. (1992) A cluster of hydrophobic amino acid residues required for fast Na^+ channel inactivation. Proceedings of the National Academy of Sciences of the United States of America 89: 10910-10914.
41. Catterall WA (2000) From ionic currents to molecular mechanisms: The structure and function of voltage-gated sodium channels. Neuron 26: 13-25.
42. Tsushima RG, Li RA, Backx PH (1997) P-loop flexibility in Na^+ channel pores revealed by single- and double-cysteine replacements. Journal of General Physiology 110: 59-72.
43. Hallegraeff GM (1993) A review of harmful algal blooms and their apparent global increase Phycologia 32: 79-99.
44. Kao C (1966) Tetrodotoxin, saxitoxin and their significance in the study of excitation phenomena. Pharmacological Reviews 18: 977-1049.
45. Gawley RE, Rein KS, Kinoshita M, Baden DG (1992) Binding of brevetoxins and ciguatoxin to the voltage-senstive sodium-channel and conformational analysis of brevetoxin-B. Toxicon 30: 780-785.
46. Dechraoui M-Y, Naar J, Pauillac S, Legrand A-M (1999) Ciguatoxins and brevetoxins, neurotoxic polyether compounds active on sodium channels. Toxicon 37: 125-143.
47. LePage KT, Baden DG, Murray TF (2003) Brevetoxin derivatives act as partial agonists at neurotoxin site 5 on the voltage-gated Na+ channel. Brain Research 959: 120-127.
48. Dravid SM, Baden DG, Murray TF (2004) Brevetoxin activation of voltage-gated sodium channels regulates Ca^{2+} dynamics and ERK1/2 phosphorylation in murine neocortical neurons. Journal of Neurochemistry 89: 739-749.
49. Jeglitsch G, Rein K, Baden DG, Adams DJ (1998) Brevetoxin-3 (PbTx-3) and its derivatives modulate single tetrodotoxin-sensitive sodium channels in rat sensory neurons. Journal of Pharmacology and Experimental Theraputics 284: 516-525.
50. Trainer VL, Baden DG, Catterall WA (1994) Identification of peptide components of the brevetoxin receptor site of rat brain sodium channels. Journal of Biological Chemistry 269: 19904-19909.
51. Satake M, Campbell A, Van Wagoner RM, Bourdelais AJ, Jacocks H, et al. (2009) Brevisin: an aberrant polycyclic ether structure from the dinoflagellate *Karenia brevis* and its implications for polyether assembly. The Journal of Organic Chemistry 74: 989-994.
52. Lee MS, Qin G, Nakanishi K, Zagorski MG (1989) Biosynthetic studies of brevetoxins, potent neurotoxins produced by the dinoflagellate *Gymnodinium breve*. Journal of the American Chemical Society 111: 6234-6241.

53. Zhou Y, Pan F-G, Li Y-S, Zhang Y-Y, Zhang J-H, et al. (2009) Colloidal gold probe-based immunochromatographic assay for the rapid detection of brevetoxins in fishery product samples. Biosensors and Bioelectronics 24: 2744-2747.
54. Baden DG (1989) Brevetoxins-unique polyether dinoflagellate toxins. FASEB Journal 3: 1807-1817.
55. Baden D, Bourdelais AJ, Jacocks H, Michelliza S, J. N (2005) Natural and derivative brevetoxins: historical background, multiplicity, and effects. Environmental Health Perspectives 113: 621-625.
56. Keeling PJ (2004) Diversity and evolutionary history of plastids and their hosts. American Journal of Botany 91: 1481-1493.
57. Baldauf SL (2003) The deep roots of eukaryotes. Science 300: 1703-1706.
58. Armbrust EV, Berges JA, Bowler C, Green BR, Martinez D, et al. (2004) The genome of the diatom *Thalassiosira pseudonana*: Ecology, evolution, and metabolism. Science 306: 79-86.
59. Oami K (2004) Correlation between membrane potential responses and tentacle movement in the dinoflagellate *Noctiluca miliaris*. Zoological Science 21: 131-138.
60. Eckert R, Sibaoka T (1968) The flash triggering action potential of the luminescent dinoflagellate *Noctiluca*. The Journal of General Physiology 52: 258-282.
61. Taylor AR (2009) A Fast Na^{+}/Ca^{2+} Based Action Potential in a Marine Diatom. PLoS ONE 4: e4966.
62. Taylor AR, Brownlee C (2003) A novel Cl^{-} inward-rectifying current in the plasma membrane of the calcifying marine phytoplankton *Coccolithus pelagicus*. Plant Physiology 131: 1391-1400.
63. Ren DJ, Navarro B, Xu HX, Yue LX, Shi Q, et al. (2001) A prokaryotic voltage-gated sodium channel. Science 294: 2372-2375.

CHAPTER TWO

MOLECULAR INVESTIGATION OF VOLTAGE-GATED ION CHANNELS IN CHROMALVEOLATES

Prepared in the style of PLoS Biology

Abstract

Voltage-gated sodium channels play an important role in physiological function associated with membrane excitability and cellular signaling. They are believed to have arisen in animals possessing primitive neuromuscular systems of the unikont eukaryotic lineage. Recent biophysical and genomic evidence supports more widespread presence of four-domain voltage-gated Na^+ and Ca^{2+} channels in unicellular organisms of both plantae and chromalveolate lineages. A bioinformatics search was conducted to expand our current view on VGC evolution in the unicellular eukaryotes with emphasis on the chromalveolates. Available genomes were surveyed for genes encoding homologues to the single domain bacterial Na^+ channel, the two pore Ca^{2+} channel and four pore Na^+ and Ca^{2+} channels. The homology search revealed several chromalveolate VGCs that appear to be highly conserved in the functional domains which include the voltage sensor and pore selectivity filter of the protein. Our phylogenetic analysis supports a chromalveolate VGC clade within the Ca^{2+} channel sequences with apparent loss of the four domain VGCs in some diatoms and alveolates. The results presented here further support the presence of four domain VGCs early in eukaryote evolutionary history and the retention of VGCs in unicellular chromalveolates. These VGCs likely play a significant role in the physiology, cell signaling and sensory ecology of marine chromalveolates and could conceivably be a target for marine toxins known to interact with VGCs in animals.

Introduction

Chromalveolata includes four major clades, the cryptophytes, haptophytes, stramenopiles, and alveolates including the ciliates, apicomplexians and dinoflagellates, which encompass the dominant taxa of marine plankton. These protists demonstrate diverse morphology and modes of

nutrition that have led their evolutionary success. They make up a monophyletic eukaryotic supergroup based on plastid evolution. The chromalveolate hypothesis proposes that plastids arose once via the endosymbiosis of cyanobacteria and have subsequently been laterally transferred to the last common ancestor of the chromalveolates via secondary endosymbiosis of a red alga [1,2,3,4,5]. However, the validity of this hypothesis has been challenged by genomic analysis of the stramenophiles *Thalassiosira pseudonana* and *Phaeodactylum tricornutum* showing greater presence of green algae genes compared to red algae genes, that predate the split of basal chromalveolate clades, in the diatom genome [6]. These findings suggest that there were three endosymbiosis events with secondary endosymbiosis of green alga predating the red algal capture in chromalveolate. Nevertheless, these protists are a chimera of animal, green and red alga genes.

Interestingly, genomic analysis of *Thalassiosira pseudonana* revealed that 806 protein encoding genes aligned only with heterotrophic endosymbiont representative mouse sequences suggesting that these genes were derived from the heterotrophic endosymbiont host [4]. During the endosymbiotic events that gave rise to the chromalveolates, the "animal-like" genes were conserved in a primary host nuclear genome and may have been retained in multiple eukaryotic groups. Among these proteins, the Na^+/Ca^{2+} voltage-gated channels (VGCs) which underlie fundamental physiological processes such as cellular homeostasis, cellular signaling, cell motility and membrane excitability appear to be a case in point[7,8].

VGCs belong to a superfamily of pore forming proteins consisting of K^+, Ca^{2+} and Na^+ channels. The simplest channels are the K^+ channels, ranging from one domain made up of two α-helical transmembrane (TM) segments to 6TM designated S1-S6 [9]. Bacterial Na^+ channels

(NavBac) are comprised of a single domain with 6TM [10]. It has been proposed that gene duplication events occurred within this family during evolution of the ion channels and subsequent mutations have led to altered selectivity and biophysical characteristics among the related families [9,11,12]. The two-pore Ca^{2+} channel (TPC) is composed of two homologous domains as a result of gene duplication and has been characterized in both plant [13] and animal [14] tissues. The TPC could be the link, via a second round of duplication, between the ancestral prokaryotic single domain channel and the larger four domain VGC proteins in the superfamily. Thus, the large four domain proteins which form two major groups, the Ca^{2+} and Na^{+} VGCs, may have arisen from two cycles of gene duplication originating from an ancestral bacterial one-domain channel [15,16].

The primary functional characteristics of VGC proteins include: ion permeation pathway, gating mechanism and regulation [11]. A highly conserved feature of all the VGCS is the S4 segment of each transmembrane domain that contains positively charged arginine residues [9]. The S4 acts as the voltage sensor for channel activation [17]. In four domain channels, pore selectivity is controlled by critically conserved residues between S5 and S6 of each TM unit, forming the P-loop [11,18]. In animal Ca^{2+} and Na^{+} selective VGCs the consensus pore filter is EEEE and DEKA respectively [18]. Conserved amino acid residues also regulate the inactivation of these channels [19].

Voltage activated Ca^{2+} and Na^{+} channels play a key role in rapid action potential based cellular signaling associated with neuromuscular function. Until recently it was believed that only complex multicellular metazoans [20,21,22] exhibited the rapid membrane excitability associated with the Na^{+}/Ca^{2+} VGC family, however, biophysical evidence for fast Na^{+}/Ca^{2+}

based action potentials prior to the divergence of the opisthokonts is accumulating [8,16,23]. The bioluminescent dinoflagellate *Noctiluca miliaris* exhibits fast (ms) action potentials that trigger scintillon flashes and regulate the rapid coiling of the feeding tentacle [24,25]. Moreover, diatoms and coccolithophorids have recently been shown to have excitable membranes that respond to membrane depolarization by generating fast "animal-like" action potentials. The biophysical features include a fast (milliseconds) inward current followed by a rapid (seconds) repolarization of the membrane [8,23]. The pharmacological properties of the diatom VGCs closely resemble those of cardiac-type Na^+/ Ca^{2+} channels [8]. Genomic analysis also supports the contention that the evolution of the four domain VGCs that underpins these action potentials lies much deeper within the eukaryotes than has been previously suspected [8,10].

Given the emerging and widespread biophysical evidence of membrane excitability in many protists including the chromalveoltates, my hypothesis is that four domain Na^+/Ca^{2+} VGCs are likely to have arisen early in eukaryote evolution and have subsequently been retained in multiple lineages including the chromalveolates. To examine this hypothesis more closely, an *in silico* analysis of newly available genomic databases representative of the major eukaryotic clades was conducted. The key characteristics of the four- domain Na^+/Ca^{2+} VGCs, including the pore domains and inactivation filter were compared. This search revealed a loss of the four-domain VGC in two of three diatom genomes investigated. The phylogenetic relationships among the putative VGC genes from the chromalveolates, excluding *Emilana huxleyi*, showed more similarity to the four domain Ca^{2+} channels.

Results

Bioinformatic investigation of VGC family evolution

Analyses of eukaryote genomes resulted in an interesting distribution of NavBac, TPC and four domain Na^+/Ca^{2+} VGCs that appear to be present in three of the five supergroups defined by Keeling (2004) [1]: plantae, chromalveolates and unikonts (Table 3). Within the supergroups possessing VGCs, Rhodophyta, Apicomplexans, Cryptomonads, and Amoebozoa examined appear to have lost the Na^+ or Ca^{2+} VGCs (Table 3). Examination of genomes from two other supergroups (rhizaria and excavates) failed to reveal any homologous sequences to the protein BLAST queries.

A BLASTP search of *Aureococcus anophagefferens, Ectocarpus siliculosis, Fragilariopsis cyclindrus , Thalassiosira pseudonana* and *Phaeodactylum tricornutum* genomes revealed genes possessing two conserved domains both of which contained six transmembrane segments, a voltage sensor and pore loop. These two domain genes shared homology to the two pore calcium channel AtTPC1 in *Arabidopsis thaliana* [13] and TPCI in *Rattus norvegicus* kidney [14]. The embryophyte *Physcomitrella patens* also possesses a gene coding for a TPC. Homologues to the single domain NavBac channel [10] were only found in three bacillariophytes: *P. tricornutum , F. cyclindrus* and *T. pseudonana*.

Of the protein sequences that showed high homology to characterized unikont Na^+ VGCs, a multiple sequence amino acid alignment was generated by Clustal W. The alignment of putative protein sequences for four-domain VGCs in chromalveolates showed similar conserved regions as the metazoan VGCs (Figure 1 and Figure 2, grey). The pore region with inner residues

of the selectivity filter is present in the chromalveolates (Figure 1, black) and plantae (not shown). The inner filter of these two groups closely resembles the Ca^{2+} channel EEEE filter, except for *E. huxleyi* with a DEED filter and *Tetrahymena themophilia* with an EENE filter. The outer pore residues (Figure 1, orange) which are highly conserved in metazoa Na^{+} VGC (EEMD) are not conserved in the chromalveolates. A cluster of hydrophobic amino acid residues between domains 3and 4 has been found to play a critical role in controlling the inactivation gating mechanism of the Na^{+} VGC [19]. The so called inactivation domain comprising the amino acid motif IFM does not seem to be a well conserved in the chromalveolates.

A phylogentic tree constructed using the Minimum Evolution method [26] and based on the VGC sequence alignment provides insight into the unique evolutionary placement of the chromalveolate and plantae VGCs (Figure 3). Included in the alignment are well characterized Na^{+} and Ca^{2+} four-domain channels used to determine placement of identified putative eukaryotic proteins. The tree supports the divergence of the characterized unikont Na^{+} and Ca^{2+} VGC genes into two distinct clades (Figure 3) [20,21,22]. The plantae, represented by sequences from the unicellular green algae *C. reindhardtii, M. pusilla,* and *O. lucimarinu* branched off into two nodes, both nested in Ca^{2+} clade but with weak bootstrap support. The chromalveolate sequences also branched off in the Ca^{2+} clade (bootstrap = 88), with the stramenophiles *T. pseudonana* and *E. siliculosus* grouped together (bootstrap = 59) and forming a larger node with the *Phytophthora* spp. (bootstrap = 99) resulting in a chromist group. *E. huxleyi* putative sequences showed significant divergence from other eukaryote Na^{+} and Ca^{2+} VGC sequences acting as an outgroup of the phylogenetic tree (Figure 3). Resolution of the placement of chromalveolate and plantae VGCs in the tree was limited by taxon sampling and will be improved as more eukaryotic genomes become available.

Discussion

Voltage-Gated Ion Channels in Chromalveolates and other Eukaryote Lineages

The results suggest that representatives of the VGC supergroups are found in at least three out of the five major eukaryotic supergroups, providing support for the hypothesis for deep evolutionary roots of this ion channel family. While the presence of many four domain VGCs was expected in the unikonts, the analysis revealed the presence of Na^+ VGCs in organisms that predate the appearance of the first neuromuscular systems, such heterotrophic single-celled choanoflagellate *Monosiga brevicollis. M. brevicollis* is closest unicellular relative to the animal phyla and can provide important insight into the evolutionary changes of Na^+/Ca^{2+}VGCs in this group. Interestingly, in the plantae, four domain Na^+/Ca^{2+}VGC genes were found in the prasinophytes *Micromonas pusilla* and *Ostreococcus lucimarinus* with high homology to four domain Ca^{2+} VGCs. Voltage-gated Ca^{2+} channels were also found in the chlorophyte, *Chlamydomonas reindhardtii*, however, the same putative gene could not be found in the chlorophyte *Volvox carteri f. nagariensis.*

In the chromalveolates, representative species from the ciliates, oomycetes, bacillariophytes, brown algae, haptophytes and alveolates (*Perkinsus marinus*) show homologues to the "animal-like" Na^+/Ca^{2+} four domain VGCs. This supports the hypothesis of a deep evolutionary origin of these channels and associated cellular signaling. Interestingly, the apicomplexians and excavates appear to have lost the four domain VGC genes and this may be as a result of genomic reduction associated with their adaptation to a parasitic lifestyle [27,28,29]. The biophysical evidence for the bacillariophytes suggests that the four-domain VGC selectivity filter, which is more like a Ca^{2+} channel, is not as highly selective as the animal Na^+

channels [8]. Given evidence for a green alga lineage prior to the red alga endosymbiotic event in the bacillariophytes [6], it is possible that VGC genes in the chromalveolates may have been acquired via both vertical (host) or endosymbiont transfer (green or red algal lineages).

From the phylogenetic analysis presented, the VGC genes of chromalveolates (with the exception of the haptophyte *E. huxleyi*) appear to be more closely related to the four domain Ca^{2+} channels. This is supported by the presence of a conserved EEEE selectivity filter in the pore loop, which in the unikont VGCs are characteristic of Ca^{2+} permeation. This implies that functional VGC proteins derived from the chromalveolate genes likely mediate rapid Ca^{2+} influx when activated. The key residues critical for rapid inactivation [19,30] of Na^{+} VGCs do not appear to be conserved in the chromalveolates implying altered inactivation kinetics in these channels potentially slowing the repolarization of the membrane and prolonging the action potential. However, the amino acid residues present at the inactivation site are very similar in polarity and size to those of the inactivation motif characterized in animal Na^{+} channels, so the functional consequences of the apparent lack of conservation in the chromalveolate VGCs may not be that significant. The variability of the pore domains and inactivation gate implies that the specificity of the residues that control permeability and gating of Na^{+} and Ca^{2+} VGCs requires re-examination.

Diatoms are known to live in close association with bacteria on their frustules, so the presence of NavBac channels in bacillariophytes could be a result of direct horizontal gene transfer. Horizontal gene transfer is the movement of genetic material between different species and is believed to contribute significantly to protist genomes [31]. Genome analysis of *P. tricornutum, T. pseudonana, Emiliana huxleyi, Plasmodum falciparum,* and *Guillardia theta* and

analysis of *K. brevis* EST library provide support for the co-occurrence of prokaryote derived genes encoding the same enzymes in distantly related eukaryotic lineages [4,6,31,32,33].

Although a putative VGC gene was not found in the representative of the rhizaria (*Bigelowiella natans)*, there has been little molecular work conducted on this group thus far, and it would be premature to draw conclusions until more rhizaria genomes are available. As with the rhizaria, more genomic data is required for all the eukaryotic groups examined here. Nevertheless, it is clear that four-domain Na^+/Ca^{2+} VGCs are found throughout the evolutionary tree, but have been lost in embryophytes and parasitic apicomplexans and excavates where rapid signaling may no longer be required. Based on the long evolutionary divergence of the respective supergroups and sub-taxa it is unlikely that these channels co-evolved among the different lineages, but rather were retained or loss from a common eukaryotic ancestor.

In conclusion, our analysis shows numerous eukaryotic lineages, including several chromalveolates, possess VGCs that likely play an important role in cellular homeostasis and signaling. This is consistent with biophysical evidence of VGCs in chromalveolates [8,23,25] and unicellular plantae [34]. This analysis provides further support for deep-rooted origin of VGCs in the Eukaryota. Finally, the presence of four domain Na^+/Ca^{2+} VGCs in aquatic protists raises the intriguing possibility that such organisms may be affected by algal neurotoxins such as brevetoxins and saxitoxins [35,36,37] that are characterized by their interaction with animal Na^+ VGCs [38,39].

Materials and Methods

Alignment of Eukaryote Amino Acid Sequences and Phylogenetic Analysis

A selection of available eukaryote genomes from all major groups including the unikonts, rhizaria, plantae, excavates and chromalveolates were accessed from both NCBI and JGI Genome Databases. A BLASTP search [40] was conducted with the amino acid sequences of known animal and protist four domain VGCs (*L. bleekeri* BAA03398, *R. norvegicus* AAA41682, and *T. pseudonana* XP_002289136) , two pore domain VGCs (A. *thaliana* AAD11598 and *R. norvegicus* BAA76556) and the NavBac channel of *T. pseudonana* (XP_002287819) as queries. Hits with expect values of $\leq 10^{-20}$ were subsequently used in the analysis. A multiple sequence alignment was performed with ClustalW [41] in the Molecular Evolutionary Genetics Analysis (MEGA 4.0) software[42] using all of the resultant protein or translated nucleotide sequences. Phylogeny was estimated using the Minimum Evolution method [26] with complete deletion of gaps in the MEGA 4.0 software [42]. Branch support was estimated from 10,000 bootstrap replicate samples with those less than 50% collapsed [43].

Table 1. Genomic evidence for voltage-gated Na^{+} or Ca^{2+} channels.

			Voltage Gated Ion Channels					
Group	**Subgroup**	**Taxon**	**1 domain**	**2 domain**	**4 domain**	**Protein Accession Number**	**E value**	**References**
Rhizaria	Cercozoa	*Bigelowiella natans*	-	-	-			
Plantae	Chlorophytes	*Chlamydomonas reindhardtii*	-	-	+	206627‡; 194450‡	1.0E-111	[44]
		Micromonas pusilla	-	-	+	48447‡; 95305‡; 32293‡; 84447‡; 82714‡; 21063‡	1.0E-127	
		Volvox carteri f. nagariensis	-	-	-			
		Ostreococcus lucimarinus	-	-	+	32140‡	1.0E-129	
	Rhodophyta	*Cyanidioschyzon merolae*	-	-	-			
		Galdieria sulphuraria	-	-	-			
	Bryophyta	*Physcomitrella patens*	-	+	-	BAF34917†	0.0	
	Viridplantae	*Arabidopsis thaliana*	-	+	-	AAD11598†	0.0	[68]
Excavates	Parabasalids	*Trichomonas vaginalis*	-	-	-			
	Kinetoplastids	*Trypanosoma cruzi*	-	-	-			
	Euglenozoa	*Leishmania major strain*	-	-	-			
	Diplomonads	*Giardia lamblia*	-	-	-			
	Heterolobosea	*Naegleria gruberi*	-	-	-			
Chromalveolates	Apicomplexans	*Cryptosporidium parvum*	-	-	-			
		Eimeria tenella str. Houghton	-	-	-			
		Plasmodium falciparum	-	-	-			
		Theileria annulata	-	-	-			

Table 1. Continued.

Group	Subgroup	Taxon	Voltage Gated Ion Channels			Protein Accession Number	E value	References
			1 domain	2 domain	4 domain			
		Toxoplasma gondii	-	-	-			
		Babesia bovis T2Bo	-	-	-			
	Ciliates	*Paramecium tetraurelia*	-	-	+	CAK62390, CAK91591†	9.0E-119	
		Tetrahymena thermophila	-	-	+	EAR95184†	2.0E-75	
	Oomycetes	*Phytophthora infestans*	-	-	+	03693‡	0.0	
		Phytophthora capscis	-	-	+	36518‡	0.0	
		Phytophthora sojae	-	-	+	132791‡	0.0	
	Bacillariophytes	*Phaeodactylum tricornutum*	+	+	-	XP_002186055† (1D), XP_002176296† (2D)	2.0E-28, 1.0E-58	
		Fragilariopsis cyclindrus	+	+	-	197275‡(1D), 22515‡(2D)	1.0E-159, 3.0E-43	
		Thalassiosira pseudonana	+	+	+	XP_002287819† (1D), EED96127† (2D), XP_002289136† (4D)	7.0E-31, 6.0E-50, 0.0	
	Phaeophyceae	*Ectocarpus siliculosis*	-	+	+	Esi0009_0041(2D), Esi0029_0129 (4D)	7.0E-50, 1.0E-127	
	Haptophytes	*Emiliania huxleyi 1516*	-	-	+	468996‡; 448526‡	7.00E-93	
	Pelagophytes	*Aureococcus anophagefferens*	-	+	-	10203‡	4.00E-85	
	Cryptomonads	*Guillardia theta*	-	-	-			
	Perkinsea	*Perkinsus marinus*	-	-	+	EER08208†	1.00E-72	
Unikonts	Mycetozoa	*Dictyostelium discoideum*	-	-	-			
		Physarum polycephalum	-	-	-			

Table 1. Continued.

Group	Subgroup	Taxon	Voltage Gated Ion Channels			Protein Accession Number	E value	References
			1 domain	2 domain	4 domain			
	Archamoebae	*Entamoeba histolytica*	-	-	-			
	Centramoebida	*Acanthamoeba castellanii*	-	-	-			
	Choanoflagellates	*Monosiga brevicollis*	-	-	+	XP_001743090†	4.0E-150	
	Fungi	*Saccharomyces cerevisiae*	-	-	+	NP_011733†	4.0E-30	[45]
	Metazoa	*Polyorchis penicillatus*	-	-	+	AAC38974†	0.0	[46]
		Trichoplax adhaerens	-	-	+	XP_002110570†	4.0E-165	[47]
		Aiptasia pallida	-	-	+	AAB96953†	0.0	[48]
		Loligo bleekeri	-	-	+	BAA03398†	0.0	[70]
		Aplysia califonica	-	-	+	AAC47457†	0.0	[49]
		Drosophila melanogaster	-	-	+	AAB59195†	0.0	[71]
		Takifugu rubripes	-	-	+	BAA07195†	5.0E-173	[50]
		Danio rerio	-	-	+	AAG18440†	0.0	[51]
		Gallus gallus	-	+	+	XP_415322† (2D),	0.0	
						XP_422021† (4D)	0.0	
		Mus musculus	-	+	+	AAH58951† (2D),	0.0,	[52]
						CAA70325† (4D)	0.0	
		Rattus norvegicus	-	+	+	BAA76556† (2D),	0.0,	[69], [53]
						AAA41682† (4D)	0.0	
		Homo sapiens	-	+	+	AAI50204† (2D),	0.0,	[54], [72]
						CAA58042† (4D)	0.0	

† Accession number from National Center for Biotechnology Information (http://www.ncbi.nlm.nih.gov/)

‡ Accession number from DOE Joint Genome Institute (http://www.jgi.doe.gov/)

ˆ Accession number from BOGAS (http://bioinformatics.psb.ugent.be/)

Figure 1. Pore domain analysis of putative Na^+/Ca^{2+} VGCs of chromalveolates. Clustal W multiple sequence alignment of the four 'p' domains of vertebrate and invertebrate Na^+ /Ca^{2+} voltage-gated channels compared with putative homologues from representative chromalveolates. Highly conserved amino acid residues are shaded grey. Selectivity of the conserved pore region is indicated by the inner (black) and outer (orange) residues. Protein sequences were obtained from NCBI and JGI with the accession numbers indicated.

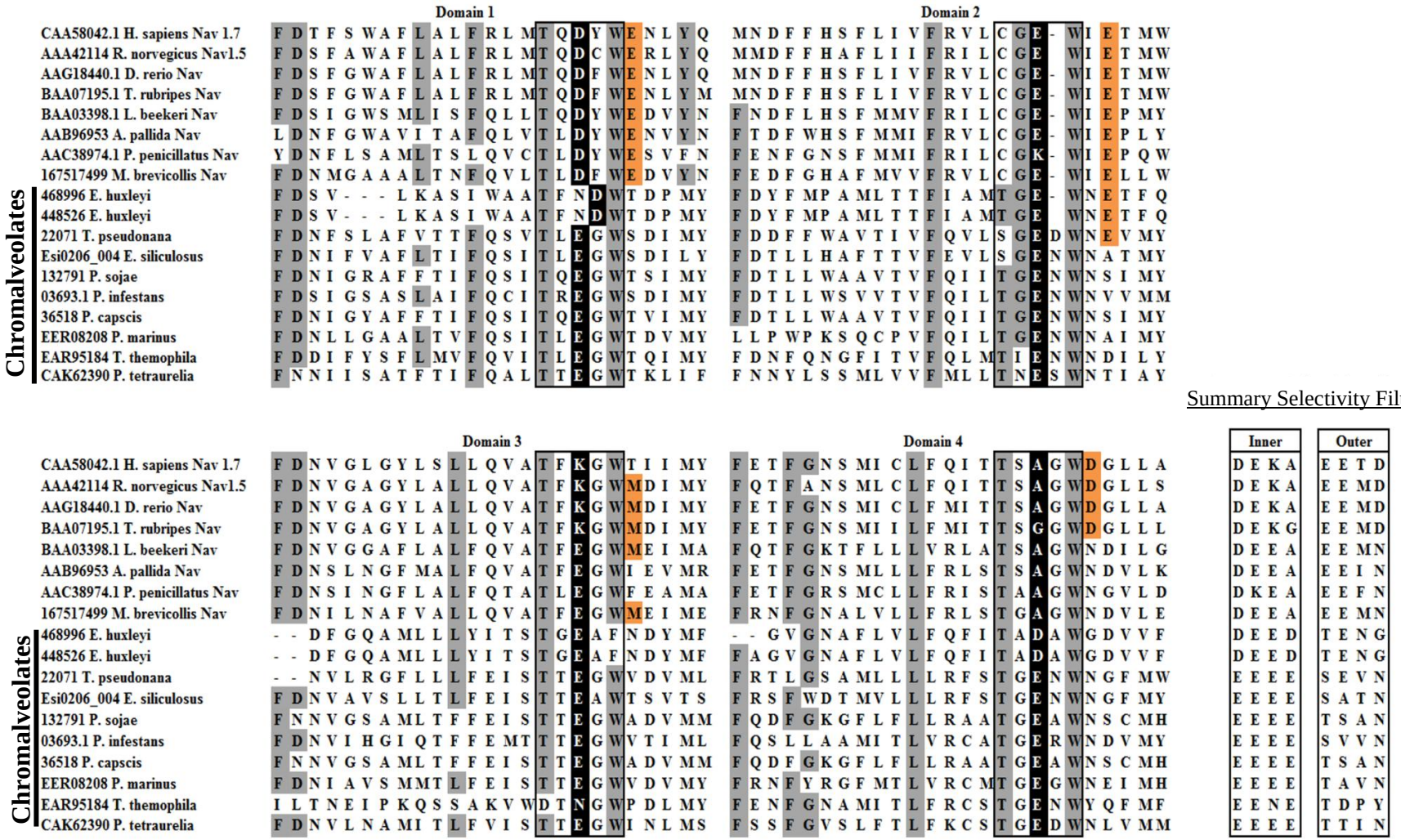

Domain 1
Domain 2
Domain 3
Domain 4
Chromalveolates
Chromalveolates
CAA58042.1 H. sapiens Nav 1.7
AAA42114 R. norvegicus Nav1.5
AAG18440.1 D. rerio Nav
BAA07195.1 T. rubripes Nav
BAA03398.1 L. beekeri Nav
AAB96953 A. pallida Nav
AAC38974.1 P. penicillatus Nav
167517499 M. brevicollis Nav
468996 E. huxleyi
448526 E. huxleyi
22071 T. pseudonana
Esi0206_004 E. siliculosus
132791 P. sojae
03693.1 P. infestans
36518 P. capscis
EER08208 P. marinus
EAR95184 T. themophila
CAK62390 P. tetraurelia
Summary Selectivity Filter
Inner
Outer
D E K A
E E T D
D E K A
E E MD
D E K A
E E MD
D E K G
E E MD
D E E A
E E MN
D E E A
E E I N
D K E A
E E F N
D E E A
E E MN
D E E D
T E N G
D E E D
T E N G
E E E E
S E V N
E E E E
S A T N
E E E E
T S A N
E E E E
S V V N
E E E E
T S A N
E E E E
T A V N
E E N E
T D P Y
E E E E
T T I N

Figure 2. Inactivation gate in chromalveolates. From the inactivation gate established in West et al. (1992), a sequence alignment of vertebrate and invertebrate Na^+ VGCs were compared with putative chromalveolate genes from a BLAST search. The highly conserved critical residues IFM (black) in vertebrates are found in the α-subunit between domain 3 and domain 4 of the Na^+ channel. Similar amino acids to the IFM filter are found in the boxed region and are highlighted light grey. All other conserved regions of the sequences are dark grey.

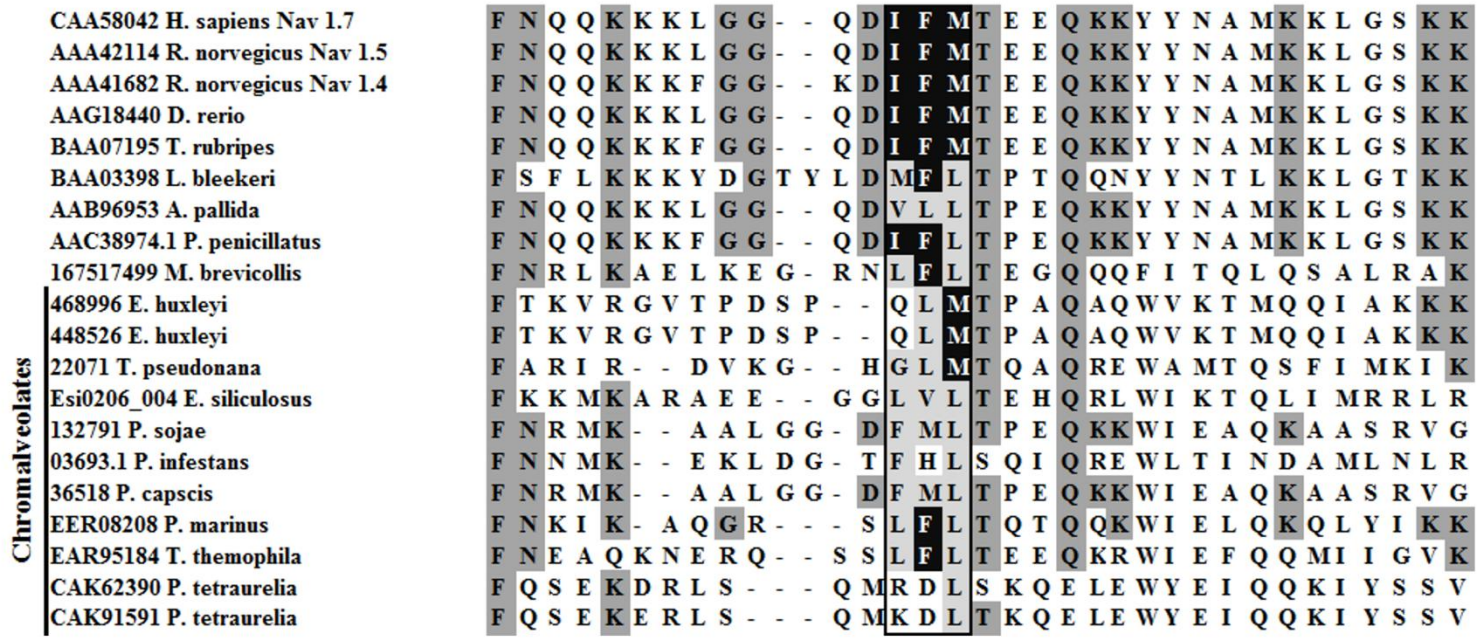
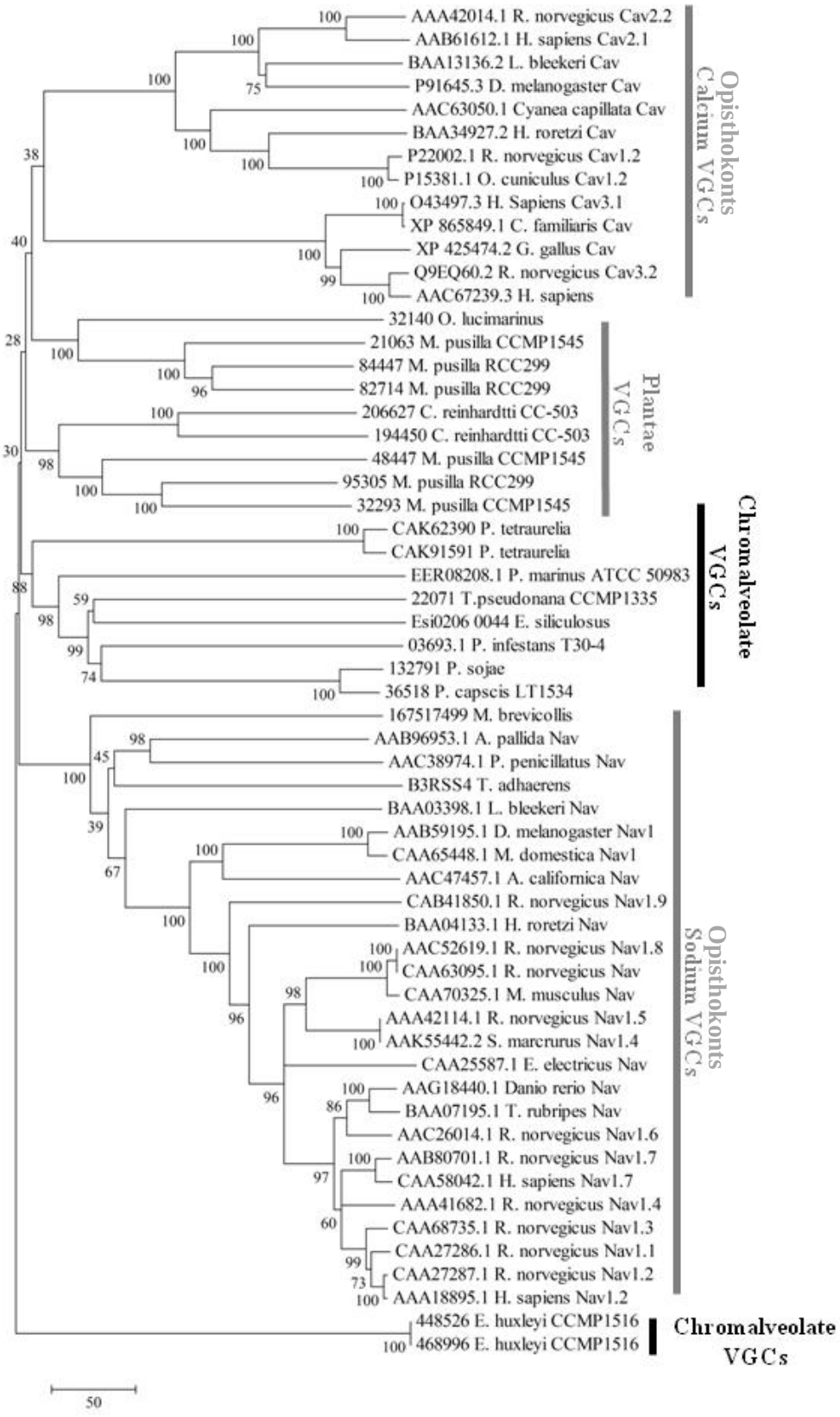

CAA58042 H. sapiens Nav 1.7
AAA42114 R. norvegicus Nav 1.5
AAA41682 R. norvegicus Nav 1.4
AAG18440 D. rerio
BAA07195 T. rubripes
BAA03398 L. bleekeri
AAB96953 A. pallida
AAC38974.1 P. penicillatus
167517499 M. brevicollis
Chromalveolates
468996 E. huxleyi
448526 E. huxleyi
22071 T. pseudonana
Esi0206_004 E. siliculosus
132791 P. sojae
03693.1 P. infestans
36518 P. capscis
EER08208 P. marinus
EAR95184 T. themophila
CAK62390 P. tetraurelia
CAK91591 P. tetraurelia

Figure 3. Phylogenetic analysis of voltage-gated Ca^{2+} and Na^{+} channels in Eukaryotes. Evolutionary relationships were inferred using the Minimum Evolution method [26]with 10,000 bootstrap replicates [55] constructed in MEGA 4.0 [42]. Percentages of replicate trees in which associated taxa cluster together under the bootstrap test are shown next to the branches. The branch lengths shown are proportional to the calculated phylogenetic distance.


AAA42014.1 R. norvegicus Cav2.2
AAB61612.1 H. sapiens Cav2.1
BAA13136.2 L. bleekeri Cav
P91645.3 D. melanogaster Cav
AAC63050.1 Cyanea capillata Cav
BAA34927.2 H. roretzi Cav
P22002.1 R. norvegicus Cav1.2
P15381.1 O. cuniculus Cav1.2
O43497.3 H. Sapiens Cav3.1
XP 865849.1 C. familiaris Cav
XP 425474.2 G. gallus Cav
Q9EQ60.2 R. norvegicus Cav3.2
AAC67239.3 H. sapiens
Opisthokonts Calcium VGCs
32140 O. lucimarinus
21063 M. pusilla CCMP1545
84447 M. pusilla RCC299
82714 M. pusilla RCC299
206627 C. reinhardtti CC-503
194450 C. reinhardtti CC-503
48447 M. pusilla CCMP1545
95305 M. pusilla RCC299
32293 M. pusilla CCMP1545
Plantae VGCs
CAK62390 P. tetraurelia
CAK91591 P. tetraurelia
EER08208.1 P. marinus ATCC 50983
22071 T.pseudonana CCMP1335
Esi0206 0044 E. siliculosus
03693.1 P. infestans T30-4
132791 P. sojae
36518 P. capscis LT1534
Chromalveolate VGCs
167517499 M. brevicollis
AAB96953.1 A. pallida Nav
AAC38974.1 P. penicillatus Nav
B3RSS4 T. adhaerens
BAA03398.1 L. bleekeri Nav
AAB59195.1 D. melanogaster Nav1
CAA65448.1 M. domestica Nav1
AAC47457.1 A. californica Nav
CAB41850.1 R. norvegicus Nav1.9
BAA04133.1 H. roretzi Nav
AAC52619.1 R. norvegicus Nav1.8
CAA63095.1 R. norvegicus Nav
CAA70325.1 M. musculus Nav
AAA42114.1 R. norvegicus Nav1.5
AAK55442.2 S. marcrurus Nav1.4
CAA25587.1 E. electricus Nav
AAG18440.1 Danio rerio Nav
BAA07195.1 T. rubripes Nav
AAC26014.1 R. norvegicus Nav1.6
AAB80701.1 R. norvegicus Nav1.7
CAA58042.1 H. sapiens Nav1.7
AAA41682.1 R. norvegicus Nav1.4
CAA68735.1 R. norvegicus Nav1.3
CAA27286.1 R. norvegicus Nav1.1
CAA27287.1 R. norvegicus Nav1.2
AAA18895.1 H. sapiens Nav1.2
Opisthokonts Sodium VGCs
448526 E. huxleyi CCMP1516
468996 E. huxleyi CCMP1516
Chromalveolate VGCs
50

References

1. Keeling PJ (2004) Diversity and evolutionary history of plastids and their hosts. American Journal of Botany 91: 1481-1493.
2. Baldauf SL (2003) The deep roots of eukaryotes. Science 300: 1703-1706.
3. Hackett JD, Anderson DM, Erdner DL, Bhattacharya D (2004) Dinoflagellates: A remarkable evolutionary experiment. American Journal of Botany 91: 1523-1534.
4. Armbrust EV, Berges JA, Bowler C, Green BR, Martinez D, et al. (2004) The genome of the diatom *Thalassiosira pseudonana*: Ecology, evolution, and metabolism. Science 306: 79-86.
5. Cavalier-Smith T (2003) Genomic reduction and evolution of novel genetic membranes and protein-targeting machinery in eukaryote-eukaryote chimaeras (meta-algae). Philosophical Transactions of the Royal Society of London Series B: Biological Sciences 358: 109-134.
6. Moustafa A, Beszteri B, Maier UG, Bowler C, Valentin K, et al. (2009) Genomic footprints of a cryptic plastid endosymbiosis in diatoms. Science 324: 1724-1726.
7. Verret F, Wheeler G, Taylor AR, Farnham G, Brownlee C (2010) Calcium channels in photosynthetic eukaryotes: implications for evolution of calcium-based signaling. New Phytologist 187: 23-43.
8. Taylor AR (2009) A fast Na^+/Ca^{2+} based action potential in a marine diatom. PLoS ONE 4: e4966.
9. Strong M, Chandy KG, Gutman GA (1993) Molecular evolution of voltage-sensitive ion channel genes: on the origins of electrical excitability. Molecular Biology and Evolution 10: 221-242.
10. Ren DJ, Navarro B, Xu HX, Yue LX, Shi Q, et al. (2001) A prokaryotic voltage-gated sodium channel. Science 294: 2372-2375.
11. Yu FH, Yarov-Yarovoy V, Gutman GA, Catterall WA (2005) Overview of molecular relationships in the voltage-gated ion channel superfamily. Pharmacological Reviews 57: 387-395.
12. Hille B (1989) Ionic channels: evolutionary origins and modern roles. Experimental Physiology 74: 785-804.
13. Furuichi T, Cunningham KW, Muto S (2001) A putative two pore channel AtTPC1 mediates Ca^{2+} flux in *Arabidopsis* leaf cells. Plant Cell Physiology 42: 900-905.
14. Ishibashi K, Suzuki M, Imai M (2000) Molecular cloning of a novel form (two-repeat) protein related to voltage-gated sodium and calcium channels. Biochemical and Biophysical Research Communications 270: 370-376.
15. Cestele S, Catterall WA (2000) Molecular mechanisms of neurotoxin action on voltage-gated sodium channels. Biochimie 82: 883-892.
16. Anderson PAV, Roberts-Misterly J, Greenberg RM (2005) The evolution of voltage-gated sodium channels: were algal toxins involved? Harmful Algae 4: 95-107.
17. Catterall WA, Goldin AL, Waxman SG (2003) International union of pharmacology. XXXIX. Compendium of voltage-gated ion channels: sodium channels. Pharmacological Reviews 55: 575-578.
18. Catterall WA (2000) From ionic currents to molecular mechanisms: The structure and function of voltage-gated sodium channels. Neuron 26: 13-25.

19. West JW, Patton DE, Scheuer T, Wang Y, Goldin AL, et al. (1992) A cluster of hydrophobic amino acid residues required for fast Na^+ channel inactivation. Proceedings of the National Academy of Sciences of the United States of America 89: 10910-10914.
20. Sato C, Matsumoto G (1992) Primary structure of squid sodium-channel deduced from the complementary-DNA sequence. Biochemical and Biophysical Research Communications 186: 61-68.
21. Loughney K, Kreber R, Ganetzky B (1989) Molecular analysis of the para locus, a sodium-channel gene in *Drosophila*. Cell 58: 1143-1154.
22. Klugbauer N, Lacinova L, Flockerzi V, Hofmann F (1995) Structure and functional expression of a new member of the tetrodotoxin-sensitive voltage-activated sodium-channel family from human neuroendocrine cells. Embo Journal 14: 1084-1090.
23. Taylor AR, Brownlee C (2003) A novel Cl^- inward-rectifying current in the plasma membrane of the calcifying marine phytoplankton *Coccolithus pelagicus*. Plant Physiology 131: 1391-1400.
24. Oami K (2004) Correlation between membrane potential responses and tentacle movement in the dinoflagellate *Noctiluca miliaris*. Zoological Science 21: 131-138.
25. Eckert R, Sibaoka T (1968) The flash triggering action potential of the luminescent dinoflagellate *Noctiluca*. The Journal of General Physiology 52: 258-282.
26. Rzhetsky A, Nei M (1992) A simple method for estimating and testing minimum evolution trees. Molecular Biology and Evolution 9: 945-967.
27. Keeling PJ (2004) Reduction and compaction in the genome of the apicomplexan parasite *Cryptosporidium parvum*. Developmental Cell 6: 614-616.
28. Wolfe KH, Morden CW, Palmer JD (1992) Function and evolution of a minimal plastid genome from a nonphotosynthetic parasitic plant. Proceedings of the National Academy of Sciences of the United States of America 89: 10648-10652.
29. Morrison HG, McArthur AG, Gillin FD, Aley SB, Adam RD, et al. (2007) Genomic minimalism in the early diverging intestinal parasite *Giardia lamblia*. Science 317: 1921-1926.
30. Ulbricht W (2005) Sodium channel inactivation: molecular determinants and modulation. Physiological Reviews 85: 1271-1301.
31. Nosenko T, Bhattacharya D (2007) Horizontal gene transfer in chromalveolates. BMC Evolutionary Biology 7: 173.
32. Andersson JO, Roger AJ (2003) Evolution of glutamate dehydrogenase genes: evidence for lateral gene transfer within and between prokaryotes and eukaryotes. BMC Evolutionary Biology 3: 14.
33. Bowler C, Allen AE, Badger JH, Grimwood J, Jabbari K, et al. (2008) The *Phaeodactylum* genome reveals the evolutionary history of diatom genomes. Nature 456: 239-244.
34. Yoshimura K (1996) A novel type of mechanoreception by the flagella of *Chlamydomonas*. Journal of Experimental Biology 199: 295-302.
35. Baden DG (1989) Brevetoxins-unique polyether dinoflagellate toxins. FASEB Journal 3: 1807-1817.
36. Van Dolah FM (2000) Marine algal toxins: Origins, health effects, and their increased occurrence. Environmental Health Perspectives 108: 133-141.
37. Kao CY (1966) Tetrodotoxin, saxitoxin and their significance in the study of excitation phenomena. Pharmacological Reviews 18: 997-1049.

38. Huang JM, Wu CH, Baden DG (1984) Depolarizing action of a red-tide dinoflagellate brevetoxin on axonal membranes. The Journal of Pharmacology and Experimental Therapeutics 229: 615-621.
39. Strachan LC, Lewis RJ, Nicholson GM (1999) Differential actions of pacific ciguatoxin-1 on sodium channel subtypes in mammalian sensory neurons. The Journal of Pharmacology and Experimental Therapeutics 288: 379-388.
40. Altschul SF, Gish W, Miller W, Myers EW, Lipman DJ (1990) Basic local alignment search tool. Journal of Molecular Biology 215: 403-410.
41. Thompson JD, Higgins DG, Gibson TJ (1994) CLUSTAL W: improving the sensitivity of progressive multiple sequence alignment through sequence weighting, position-specific gap penalties and weight matrix choice. Nucleic Acids Research 22: 4673-4680.
42. Tamura K, Dudley J, Nei M, Kumar S (2007) MEGA4: Molecular Evolutionary Genetics Analysis (MEGA) software version 4.0. Molecular Biology and Evolution 24: 1596-1599.
43. Felsenstein J (1985) Confidence limits on phylogenies: An approach using the bootstrap. Evolution 39: 783-791.
44. Fujiu K, Nakayama Y, Yanagisawa A, Sokabe M, Yoshimura K (2009) *Chlamydomonas* CAV2 encodes a voltage- dependent calcium channel required for the flagellar waveform conversion. 19: 133-139.
45. Fischer M, Schnell N, Chattaway J, Davies P, Dixon G, et al. (1997) The *Saccharomyces cerevisiae* CCH1 gene is involved in calcium influx and mating. Febs Letters 419: 259-262.
46. Spafford JD, Spencer AN, Gallin WJ (1998) A putative voltage-gated sodium channel alpha subunit (PpSCN1) from the hydrozoan jellyfish, *Polyorchis penicillatus*:structural comparisons and evolutionary considerations. Biochemical and Biophysical Research Communications 244: 772-780.
47. Srivastava M, Begovic E, Chapman J, Putnam NH, Hellsten U, et al. (2008) The *Trichoplax* genome and the nature of placozoans. Nature 454: 955-960.
48. White G, Pfahnl A, Haddock S, Lamers S, Greenberg R, et al. (1998) Structure of a putative sodium channel from the sea anemone *Aiptasia pallida*. Invertebrate Neuroscience 3: 317-326.
49. Dyer JR, Johnston WL, Castellucci VF, Dunn RJ (1997) Cloning and tissue distribution of the *Aplysia* Na^+ channel alpha subunit cDNA. DNA and Cell Biology 16: 347-356.
50. Jost MC, Hillis DM, Lu Y, Kyle JW, Fozzard HA, et al. (2008) Toxin-resistant sodium channels: parallel adaptive evolution across a complete gene family. Molecular Biology and Evolution 25: 1016-1024.
51. Tsai C-W, Tseng J-J, Lin S-C, Chang C-Y, Wu J-L, et al. (2004) Primary structure and developmental expression of zebrafish sodium channel Nav1.6 during neurogenesis. DNA and Cell Biology 20: 249-255.
52. Souslova VA, Fox M, Wood JN, Akopian AN (1997) Cloning and characterization of a mouse sensory neuron tetrodotoxin-resistant voltage-gated sodium channel gene, Scn10a. Genomics 41: 201-209.
53. Trimmer JS, Cooperman SS, Tomiko SA, Zhou J, Crean SM, et al. (1989) Primary structure and functional expression of a mammalian skeletal muscle sodium channel. Neuron 3: 33-49.

54. Brailoiu E, Churamani D, Cai X, Schrlau MG, Brailoiu GC, et al. (2009) Essential requirement for two-pore channel 1 in NAADP-mediated calcium signaling. The Journal of Cell Biology 186: 201-209.
55. Felsenstein J (1985) Confidence limits on phylogenies: An approach using the bootstrap. . Evolution 39: 783-791.

CHAPTER THREE

BREVETOXIN SENSITIVE IONIC CURRENTS IN THE MARINE DIATOM *ODONTELLA SINENSIS*

Prepared in the style of PLoS Biology

Abstract

The effects of brevetoxin, produced by the dinoflagllate *K. brevis*, were examined on the voltage activated ion currents of the non-toxic centric diatom *Odontella sinensi*s. Prior studies of brevetoxin interaction on animal Na^+ voltage-gated channels (VGCs) demonstrate high specific binding to site 5 causing membrane hyperexcitability and alteration of VGC kinetics. A bioinformatic analysis of the identified site 5 in vertebrates revealed only few conserved amino acids in putative VGC sequences from a range of chromalveolates including diatoms. Nevertheless, fluorescently labeled PbTx-B was readily taken up and specifically accumulated in the membranes, cytoplasm and lipid droplets of *O. sinensis.* To examine whether or not PbTx-3 interacted with *O. sinensis* ion channels, single electrode current and voltage clamp experiments were conducted. Current clamp recordings showed that bolus additions of 1µM PbTx-3 had no effect on free running membrane potential. Under voltage clamp, PbTx-3 inhibited the Na^+ evoked peak current by 33% with a significant positive shift in the reversal potential. The delayed outward current was inhibited by 25%. No significant change in activation kinetics was observed. However, a small, but significant, 4mV positive shift in voltage-dependent inactivation of the Na^+ channel in the presence of PbTx-3 suggests a slight change in the kinetics from the open and close conformation in these channels such that probability of opening is reduced for any given membrane voltage. Results indicate that brevetoxins are readily absorbed and accumulated by *O. sinensis* and significantly affect permeation of the Na^+ VGCs while exhibiting limited impacts on channel kinetics. The lack of homology in brevetoxin binding site 5 of the chromalveolates VGC sequences is consistent with the biophysical data, indicating that diatoms, although sensitive to relatively high concentrations of brevetoxin, may be resistant to alleopathic effects at environmentally relevant exposures.

Introduction

Marine diatoms are unicellular, photosynthetic chromalveolates of the stramenophile lineage that play a dominant role in oceanic primary production. Derived from a secondary endosymbiotic event, their genomes represent a combination of genes from the heterotrophic host and red algal endosymbiont [1,2,3]. Recent investigation of the diatom genomes *Thalassiosira pseudonana* and *Phaeodactylum tricornutum* also show a significant percent of the proteome is of green algae origins [4] suggesting a more ancient endosymbiotic event prior to the fixation of a red alga-like symbiont. Over the evolutionary history of the diatom (more than 180 mya) the chimera of genes from the different endosymbiotic events has been subject to differential loss and retention of the nuclear genes in addition to horizontal gene transfer from prokaryotes [5].

One particular gene of interest retained in *T. pseudonana* genome is a four-domain voltage-gated Na^+/Ca^{2+} channel [2]. Molecular features of the diatom *T. pseudonana* voltage-gated Na^+/Ca^{2+} channel were found to be homologous to animal Na^+ voltage-gated channels (VGCs) that underpin membrane excitability in neuromuscular systems of animals. The diatom VGC possesses four homologous domains with six transmembrane segments (S1-S6), a voltage sensor on S4 and conserved pore domains between S5 and S6 of each domain [6]. Furthermore, a functional role of these VGCs in rapid cellular signaling has been demonstrated in a biophysical examination of the centric diatom *Odontella sinensis* [7]. These cells exhibit spontaneous and evoked fast action potentials with the underlying depolarizing ionic currents possessing kinetic and pharmacological characteristics closely resembling cardiac Na^+/Ca^{2+} permeable channels of animals [7].

Na^+ VGCs in vertebrates and invertebrates can be modified or inhibited by a range of natural biological compounds that severely disrupt normal function at nM concentrations. A number of toxins from marine dinoflagellates (saxitoxin, ciguatoxin, and brevetoxin) are known to specifically interact with Na^+ VGCs. These algal toxins are thought to function as a chemical defense against predators, inter- and intraspecific competitors for resources [8,9,10,11,12,13,14], however experimental evidence to support such functional and ecological roles of these toxins is limited.

The marine dinoflagellate *Karenia brevis* produces two highly potent polyether brevetoxins (PbTx-1 and PbTx-2) intracellularly with numerous environmental derivatives. They activate the voltage-gated sodium (Na^+) channel by binding to site 5 [15,16,17,18,19]. Interaction of these toxins with animal Na^+ VGCs results in: a negative shift in the activation of potential [20], inhibition of inactivation [20,21] and an increase in Na^+ influx associated with membrane depolarization [22,23]. Periodic blooms of *K. brevis* are common in the Gulf of Mexico where they are responsible for massive fish kills, marine mammal strandings and cause neurotoxic shellfish poisoning (NSP) in humans [14,24,25,26,27], although it is unlikely that these effects represent direct allelopathy against these top predators. A more reasonable ecological target of the toxin would be planktonic predators or competitors. However, ingestion of toxic *K. brevis* cells by pelagic copepods [28,29], rotifers [10] and benthic amphipods and urchins [30] in laboratory experiments have variable effects on zooplankton growth or fecundity. Another possible target of the toxins is co-occurring phytoplankton that are actively competing for limited resources in the photic zone. Culture experiments have provided evidence for and against allelopathic interactions of *K. brevis* and its toxins with other phytoplankton [14,31,32,33]. If *K. brevis* is able to reduce the competition of co-occurring phytoplankton with

toxin interactions, this may be one of the key elements that determine bloom dynamics during red-tide events.

Based upon recent biophysical [7] and molecular evidence for Na^+/Ca^{2+} VGCs in the diatoms and other chromalveolates (see Chapter Two), a working hypothesis that brevetoxins will exert allelopathic effects on neighboring non-toxic protists by interacting with VGCs was established. Using *O. sinensis* as the diatom model, the hypothesis predicts brevetoxins will alter the activation, inactivation and subconductance properties of the Na^+ currents of this cell. In order to address this hypothesis, an *in silico* analysis comparing highly conserved brevetoxin binding site 5 in vertebrate Na^+ channels with putative diatom and other chromalveolate Na^+ VGC sequences was conducted to predict possible molecular interactions. Next, imaging of a novel brevetoxin fluorescent probe was conducted to observe how brevetoxin interacts at a cellular and subcellular level with *O. sinensis*. Finally, electrophysiological approaches were used to investigate whether brevetoxins interact at a molecular level with VGCs in *O. sinensis* to alter the biophysical characteristics of the Na^+/Ca^{2+} currents underlying membrane excitability.

Results

Brevetoxin Binding Site 5 Analysis

A multiple sequence alignment was used to investigate whether putative Na^+/Ca^{2+} VGCs of chromalveolates are conserved at the PbTx-3 binding site 5 previously characterized in the rat brain Nav1.2 [16] (Figure 1). Site 5 in metazoan VGCs is composed of two 18-20 amino acid segments on the α-subunit (Figure 1), the first segment directly following the conserved transmembrane segment (S6) of domain 1 (D1), and the second, follows transmembrane segment

5 (S5) of domain 4 (D4) [16]. Among all of the representative eukaryotic VGC sequences shown, D1 S6 and D4 S5 are conserved with high homology (Figure 1). Comparison with the associated downstream Nav1.2, the PbTx-3 binding site 5 showed high conservation in the vertebrate representatives *Danio rerio, Takifugu rubripes, Mus musculus* and *Rattus norvegicus* but significant divergence of site 5 residues in *L. bleekeri*, *M. brevicollis* and the chromalveolates.

Bodipy-PbTx-B Staining in O. sinensis and K. brevis

In control experiments, no significant internalization or fluorescence staining were observed in the presence of unreacted 400 nM PbTx-2 and unreacted 400 nM Bodipy tags. The cells experienced no loss of morphology or apoptosis during up to 2 hr incubations. (Data not shown).

The uptake of fluorescent Bodipy-conjugated-PbTx-B in *O. sinensis* showed intense uniform cytoplasmic staining after 30 min in all cells (Figure 2, 6 experiments). Within two hours, the probe remained cytoplasmic but also appeared to accumulate into distinct subcellular regions. (Figure 2B, F, G). The subcellular location of Bodipy-PbTx-B in *O. sinensis* was further investigated by careful examination of subcellular morphological features along with fluorescent organelle probes. Neither the chloroplast, which is naturally autofluorescent, the nucleus (readily observed in corresponding DIC images) nor the central vacuolar space showed significant accumulation of Bodipy-PbTx-B conjugate (6 independent experiments). Co-labeling mitochondria confirmed no uptake into the mitochondria either (n = 1 experiment, Figure 2D, H). In all cells, there was co-localization of the Bodipy-PbTx-B and Nile Red fluorescence suggesting neutral lipid bodies are the site of intense punctuate staining observed during longer

incubations (1 experiment, Figure 2L). However lipid body co-localization did account for all the subcellular Bodipy-PbTx-B staining and there were other regions of the cell unassociated with lipid bodies brightly stained.

In comparable treatments of *K. brevis* with 400nM Bodipy-conjugated-PbTx-B, no appreciable dye loading over the course of four hours was observed (4 experiments, Figure 3). However, mitochondria and neutral lipid droplets were visualized with the same organelle probes (Figure 3).

PbTx-3 Has No Effect on Resting Membrane Potential and Membrane Excitability

Under steady state conditions, *Odontella sinensis* cells exhibited endogenous membrane oscillations with spontaneous firing of rapid action potentials ranging from 50-100 ms, when the threshold voltage was reached (n = 24, Figure 5). Long periods of very stable negative membrane potentials were also observed in other cells (Figure 5C). As with the animal Na^+ VGCs, these action potentials comprised a fast rising phase followed by a slower hyperpolarization phase (Figure 4A). The cells either elicited both single or trains of action potential spikes (Figure 4A, B). In all cells examined, whether quiescent or oscillating, under current clamp stepwise injection of 1nA current over 10ms evoked an action potential (Figure 4C).

Bolus additions of ASW did not induce any deviation from the steady state recordings for up to in 15 min (n = 4, Figure 5A). Additions of 1µm PbTx-3 for 15min had no significant effect on free-running resting membrane potential in *Odontella sinensis* (n = 12). This lack of effect in the presence of PbTx-3 was regardless of mode of membrane potentials, with both spontaneous

action potentials (n = 7) and stable negative membrane voltages (n = 5) represented in the treatments (Figure 5, B and C).

PbTx-3 Inhibits O. sinensis Plasma Membrane Ion Currents

The ion currents of *O. sinensis* cells were monitored with single electrode voltage clamp recordings. A voltage-step protocol that applied depolarizing test pulses from a holding potential of -100 mV to 50 mV for 75 ms was used to activate sodium currents (Figure 6, A-D). The control bolus additions of ASW (n = 7) yielded no change in fast inward current or slower outward current after a 15 min treatment (Figure 6A, B). Addition of 1µm PbTx-3 showed a significant decrease in average peak Na^+ current amplitude from -19.7 ± 2.6nA to -13.0 ± 2.0 nA (n = 14, $p < 0.001$) after a 15min treatment (Figure 6 C, D, E). Neither voltage activation nor voltage of the peak current were significantly affected by PbTx-3 over 15 min (-47.2 ± 3.8mV and -45.7 ± 3.0mV for controls and PbTx-3 treatments respectively) (Figure 6F). Interestingly, a distinct shift in the reversal potential of the inward current from 15.0 ± 2.6 mV to 32.2 ± 5.8 mV (n = 14, $p< 0.01$) was observed suggesting a change in the selectivity of the underlying ion channels (Figure 6F). Washout with toxin-free ASW perfusion on PbTx-3 treated cells showed limited recovery after 15min (peak amplitude -14.9 ± 2.4 nA, n = 10, data not shown), and partial recovery after 30min (peak amplitude -17.6 ± 6.1, n = 4, data not shown).

The calculated percent inhibition of the ion conductance under PbTx-3 treatment was 33.6 ± 6.6% (Figure 7). Analysis of the uncharacterized outward current also showed a 25% decrease in current amplitude from 13.1 ± 1.1nA to 9. 98 ± 0.76 nA (n = 14, $p<0.001$, Figure 6F). Treatment with 1 mM lidocaine (n = 4), known to block animal and diatom Na^+ currents,

caused a 61.7 ± 7.2 % (n = 4) inhibition in the evoked Na^+ VGC of *O. sinensis* which is consistent with previous data (Figure 7)[7].

PbTx-3 Effects on Activation and Inactivation

Brevetoxins have been shown to effect both activation and inactivation properties of animal Na^+ channels [20,34]. To investigate the activation kinetics of the *O. sinensis* Na^+ VGCs in the presence of 1µm PbTx-3, ion conductance was calculated according to Strachan et al. (1999)[35] and normalized before fitting Boltzmann curves in control and PbTx-3 treatments (Figure 8). No significant change in the half activation (V_h) voltage was observed between control (-58.5 ± 1.0mV) and PbTx-3 (-57.9 ± 1.8 mV).

In order to investigate the effects of PbTx-3 on the inactivation of *O. sinensis* Na^+ current, a voltage protocol of 50 ms pre-pulses from -120mV to -35mV in 5mV increments were applied before a depolarizing pulse selected to evoke a full Na^+ current (Figure 9A, B). The peak evoked current values were normalized to the maximum peak and plotted against pre-pulse voltage before fitting a Boltzmann curve (Figure 9C). A small but significant positive shift in the half inactivation voltage (V_{inact}) was observed in the presence of PbTx-3 (-65.7 ± 0.5mV) compared to the control V_{inact} (-69.4 ± 0.5, n = 14, $p<0.05$). To further characterize the possible effects of PbTx-3 on the inactivation properties of these channels, a recovery from inactivation double pulse protocol was used (Figure 10A, B). No significant change in recovery from inactivation was observed in PbTx-3 treatments (control τ = 5.1± 0.4 and PbTx-3 τ = 6.1 ± 0.4, Figure 10C).

Discussion

Site 5 is Not Highly Conserved in Chromalveolates

Binding assays have shown that in animals brevetoxins bind with high affinity to a specific region of the Na^+ VGC termed "site 5" [15,36]. There are two components to the PbTx-3 binding site 5 on Na^+ VGC, one intracellular α-subunit (D1, S6) and one extracellular site α-subunit (D4, S5) [16]. The molecular model proposed [16] suggests that the hydrophobic brevetoxin interacts with both sites simultaneously by binding to the transmembrane interface and transversing the pore region of the Na^+ channel. Interestingly, our analysis of site 5 showed little homology in *L. bleekeri* Na^+ channel homologs although previous biophysical studies have used *L. bleekeri* axons as a model system to demonstrate the highly specific biophysical effects of brevetoxin on Na^+ channel function [20,37,38]. Therefore the identified amino acid sequences of site 5 in rat brain Nav1.2 may not represent the only brevetoxin interaction site in lower invertebrates and other eukaryotes.

Mammalian cardiac channels Nav1.5 have been shown to have substantially lower affinity for brevetoxins than nerve or skeletal muscle tissue [39,40]. However, the same reduction of binding affinity was not present in telost fish cardiac tissue [40]. Prior pharmacological experiments on *T. pseudonana* Na^+/Ca^{2+} channel showed similarity to animal cardiac channels [7] which may suggest a reduction in binding affinity and toxic interactions with this cardiac channel isoform. Evaluation of brevetoxin affinity on *T. pseudonana* and other chromalveolate Na^+ VGCs would provide more insight into the species selectivity of brevetoxins and possible resistance to brevetoxin effects.

From the comparison of site 5 in chromalveolates, there is no clear conservation of amino acid residues across this group. However, there appear to be more conserved residues in the extracellular portion of site 5. The biophysical evidence in animal Na^+ channels shows that upon interaction of brevetoxin with the pore domain, at both the intracellular or extracellular side, the activation and inactivation kinetics of the Na^+ VGCs are effected [20]. Thus, brevetoxin interaction in chromalveolate VGCs' may only involve binding to the extracellular site 5 and not the intracellular site resulting in alternate allosteric effects. Nevertheless, the critical residues for brevetoxin binding are yet to be determined and require investigation before concluding that site 5 is absent in the Chromalveolate lineage. Furthermore, given the flexibility of the brevetoxin molecule, it is not unreasonable to speculate that after binding to the more conserved extracellular receptor site, brevetoxin may interact with alternate and multiple sites within the α-subunit of the channel protein altering Na^+ channel function [16]. Examination of site 5 sequences and binding affinity assays in different chromalvolates is necessary to determine if there are specific and alternate sites with which brevetoxin interacts.

Fluorescent Brevetoxin Uptake in O. sinensis

The uptake of brevetoxin observed in *O. sinensis* indicates these lipophilic molecules are rapidly taken up by the cell where they not only remain within the cytoplasm, but also selectively accumulate in neutral lipid bodies, including lipid bodies associated with the chloroplast. Lipids are major storage product in diatoms and lipid bodies can be numerous around the cell periphery and within cytoplasmic strands [41,42]. However, distinct punctuate Bodipy-PbTx-B labeling unrelated to lipid bodies was also observed suggesting lipid accumulation cannot account for all brevetoxin uptake within the cell. The endoplasmic reticulum network, a lipid rich region of the

cell, could represent another region of Bodipy-PbTx-B uptake. Although further localization of Bodipy-PbTx-B is required to provide a better understanding of internalization and accumulation of brevetoxin, the data suggest a novel but potentially significant route of toxin transfer in microbial food webs to primary and secondary consumers.

Few experiments have addressed whether *K. brevis* is sensitive to its own toxins. Although negative consequences on cultured growth after brevetoxin addition have been observed [14,43]. From an ecological perspective, it would be disadvantageous for an organism to invest energy into production of large secondary metabolites that would cause detrimental effects to its own success. The results of the present study show that the brevetoxins do not readily enter or accumulate in *K. brevis* cells, which implies a form of resistance to their own toxins. Possible mechanisms may include breakdown of the toxin molecules at the cell surface of the dinoflagellate or novel lipid composition of the outer membranes that prevents absorption. Undoubtedly, the biophysical properties of *K. brevis* membrane need to be addressed before conclusions can be drawn about their relative resistance or sensitivity to brevetoxins.

Effects of Brevetoxin on O. sinensis Na^+ Currents

A range of studies show brevetoxins interact with animal Na^+ VGCs to cause a distinct change in membrane excitability resulting in rapid firing of action potentials generating hyperexcitability [37,38]. The underlying cause is a -10 mV shift in the voltage dependent activation of channels [22,23] and a slow recovery correlating with prolonged inactivation [19,20,34]. In the present study *Odontella sinensis* VGCs did not exhibit these characteristic changes in Na^+ channel function in the presence of 1µM PbTx-3, but did exhibit a unique interaction with the toxins resulting in reduced permeation and shift in reversal potential.

The reduction in the Na^+ peak current in *O. sinensis* was similar to that observed in squid axons [20]. It has been suggested that brevetoxins may enhance subconductance states reflecting a protein conformation in which the flow of ions through the channel pore is less efficient [34]. The slower outward rectifying current of *Odontella sinensis* action potential was also inhibited by the PbTx-3 application, which has not been described in previous studies [20,23,38]. The nature of the outward component has yet to be investigated, so it is difficult to make predictions on the inhibitory mode of action of PbTx-3 on the underlying channels. Overall, the inhibition of the diatom plasma membrane currents by PbTx-3 may have an effect on the amplitude and time course of the diatom action potential, which could potentially lead to inefficient intracellular signaling. Until the function of action potential signaling is fully examined in *O. sinensis*, it is difficult to determine to what degree the brevetoxin inhibition of the underlying currents effects sensory biology of these non-toxic cells.

Another effect of PbTx-3 on Na^+/Ca^{2+} currents in *O. sinensis* was a positive shift in the reversal potential. Such a shift implies a change in the ion selectivity in favor of Ca^{2+} ions under PbTx-3 treatment. The diatom Na^+ channels are known to be permeable to Ca^{2+} [7], presumably coupling membrane excitability with intracellular signaling processes involving changes in cytoplasmic Ca^{2+} [44,45]. It is therefore possible that PbTx-3 interaction at the pore of the channel directly or allosterically alters selectivity. This effect has not been documented in previous studies on animal Na^+ selective currents, and appears to be a unique feature of brevetoxin interaction with the diatom Na^+ VGC.

The minimal effect of PbTx-3 on activation and inactivation properties of *Odontella sinensis* Na^+ currents points again to a novel interaction of these molecules with the channel.

This is consistent with the membrane voltage recordings that indicate PbTx-3 does not induce the depolarization or hyper-excitability which would be expected if voltage dependent activation and inactivation were shifted negative. Moreover, a small positive 4 mV shift in voltage-dependent inactivation may represent a slight change in the conformational state of the Na^+ channel that would result in a slightly depolarized threshold for activation. Overall, PbTx-3 effects were observed on permeation and peak amplitude of diatom VGCs, and were not accompanied by significant changes to the kinetic properties of these currents. Whether or not lower concentrations (nM) of PbTx-3 influence channel permeation and kinetic behavior requires further investigation. However, the data presented here support the contention that diatom VGCs may be targets for toxin interactions, albeit with reduced efficacy compared to the metazoan channels. This possibly reflects selection for mutations that render the diatom channels less sensitive to PbTx-3, which could fit a 'chemical arms race' model as described in other organisms.

Material and Methods

Phytoplankton Cultures

The diatom *Odontella sinensis* (PLY606) obtained from Plymouth Culture Collection at the Marine Biological Association, UK was batch cultured in 50 ml polystyrene vented flask (Cellstar, Fisher) with autoclaved and 0.2µm filtered Gulf Stream seawater enriched f/2nutrients, Guillard's vitamins and 2 mM $NaHCO_3$ [46]. Cultures were maintained in an illuminated temperature controlled incubator (Precision Scientific) at 15°C under 12:12 day:night cycle with 100 µmol m^{-2} s^{-1} light.

Karenia brevis (EPA-JR) cultures were obtained from the University of North Carolina Wilmington Harmful Algae Culture Collection and maintained as batch cultures in a 33ppt L1 medium [47] with modified trace metal composition (0.0045g $NaSeO_3$, 0.29g $FeCl_3 \bullet 6H_2O$, 6.85g H_3BO_3, 0.86g $MnCl_2 \bullet 4H_2O$, 0.06g $ZnCl_2$, 0.026g $CoCl_2 \bullet 6H_2O$)[48]. *K. brevis* were grown in an illuminated temperature controlled incubator (Precision Scientific) at 22°C under 50µmol m^{-2} s^{-1} light on a 12:12 hour day: night cycle.

All experiments were conducted using cells collected during exponential growth phase determined by estimating cell counts of sub-samples preserved in Lugol's iodine by using a hemacytometer.

Bioinformatic Analysis of the PbTx-3 Binding Site

In order to establish genomic evidence for the presence of brevetoxin binding site 5 [16] in homologue four domain VGCs in diatoms and more broadly in the Chromalveolates, an *in silico* analysis of available genomic databases was conducted. Eukaryotic genome databases from unikonts and chromaveolates were accessed from either National Center for Biotechnology Information (NCBI) or Department of Energy Joint Genome Institute (JGI). A BLAST search [49] was conducted using amino acid sequences of four domain VGCs from animals (*L. bleekeri* BAA03398, *R. norvegicus* AAA41682) and the diatom protist *T. pseudonana* (XP_002289136) as queries. A multiple sequence alignment on the resultant hits was derived using CLUSTALW [50] in the Molecular Evolutionary Genetics Analysis (MEGA 4.0) software [51] . For all sequences obtained, the PbTx-3 binding site 5 presented in Trainer et al. (1994) was located in the resulting alignment.

Live Cell Imaging of Bodipy-PbTx-B in O. sinensis and K. brevis

Novel fluorescent conjugates of PbTx-B and Bodipy (D2371) were a generous gift received from Dr. D.G. Baden's Lab at the University of North Carolina Wilmington-Center for Marine Science. Bodipy-PbTx-B was prepared as a 1 mM stock in DMSO. An intermediate stock 10x the final loading concentration was prepared in artificial seawater (ASW-450mM NaCl, 8mM KCl, 30mM $MgCl_2 \bullet 6H_2O$, 16mM $MgSO_4 \bullet 7H_2O$, 10mM $CaCl_2$, and 5mM HEPES; pH 8.0) with the final loading concentration of 400 nM.

MitoTracker Orange CMTMRos (Invitrogen, Carlsbad, USA), a cell-permeant probe for labeling mitochondria, and Nile Red (Polysciences, Inc., Warrington, USA), a selective fluorescent stain for intracellular neutral lipid droplets were used to investigate subcellular localization of Bodipy-PbTx-B. MitoTracker Orange CMTMRos was prepared as a 1 mM stock in DMSO from which an intermediate stock or 5 µm was made in ASW and used to prepare a final loading concentration of 50 nM. Nile red was prepared as a 1mg/ml stock solution in acetone and further diluted to 100 µg/ml. The final loading concentration in ASW was 100 ng/ml.

Aliquots of both *O. sinensis* and *K. brevis* were incubated in 400 nM Bodipy-PbTx-B (*O. sinensis* n = 6, *K. brevis* n = 4) plus the fluorescent organellar probes for 15 min to 4 hrs in the dark at 20°C. Control incubations in the presence of 400 nM unreacted Bodipy (n = 2) and 400 nM unreacted PbTx-2 (n = 2) were conducted for each species to verify that there was no autofluorescence or non-specific uptake of Bodipy-PbTx probes.

Following incubation, the cells were plated out on poly-L-lysine coated 35mm glass bottom dishes (MatTek Corporation, Ashland, USA) and viewed on the Olympus Fluoview 1000 confocal microscope (Olympus, Center Valley, USA). The motile *K. brevis* cells were given pulses of shear stress and coated with 0.5% methylcellulose [52] prior to plating to limit movement during imaging. The argon 488nm laser at 1% intensity was used for excitation of both Bodipy-PbTx-B and Nile Red. MitoTracker Orange CMTMRos was excited with the 543 nm helium laser at 1% intensity. The emission bandpass filters were: Bodipy-PbTx-B 500-530 nm, MitoTracker Orange CMTMRos 560-620 nm, Nile Red 580-610 nm. Data analysis was conducted using the confocal acquisition software FV10-ASW 1.7 Viewer (Olympus, Center Valley, USA) with final image processing in GIMP 2 (GNU Image Manipulation Program).

Single Electrode Current and Voltage Clamp Recordings and Analysis

The equipment set up and protocols used in these experiments are similar to those described by Taylor (2009)[7]. Microelectrodes were fabricated from GC150F-10 thick walled borosilicate glass capillaries (Harvard Apparatus, Kent, UK) using the Flaming/Brown Micropipette Puller P-97 (Sutter Instruments, Petaluma, USA) and coated with beeswax to reduce stray capacitance. Electrodes were filled with 1 mM KCl and only those with tip resistance between 8-14 MΩ were used. This range of tip resistance was previously established to minimize cell damage while providing optimal current and voltage clamp recordings [7]. Electrodes were inserted into the headstage of an Axoclamp 900A amplifier (Axon Instruments, Union City, USA) mounted on a Sutter MP285 motorized micromanipulator (Sutter Instruments, Petaluma, USA) attached to an inverted microscope (Nikon Diaphot, Nikon, USA)

The single electrode current clamp and voltage clamp experiments were controlled using a PC connected to the amplifier via a Digidata 1200A interface (Axon Instruments, Union City, USA). An external gain was applied proper to A-D conversion using a DC amplifier (LBF-100B, Warner Instrument Corps, Hamden, USA). Data were acquired using Clampex 10.2 and all analysis was conducted offline with Clampfit 10.2 software (Axon Instruments, Union City, USA).

The pharmacological agents used during electrophysiological recordings were prepared as follows. Because 400 nM Bodipy-PbTx-B showed significant staining in 30 min, a 1μM concentration of PbTx-3 was used in all electrophysiological experiments to ensure effect would be detected during a typical recording of about 45 mins. Purified brevetoxin PbTx-3 (Lot #102008) in 0.001 mg vials were provided as a kind gift from Dr. D.G. Baden's Lab at the University of North Carolina Wilmington Center for Marine Science, Wilmington, NC. PbTx-3 was prepared as a 1 mM stock solution in DMSO and stored at -20°C. A final stock was made up in ASW to a concentration of 2 μM. Lidocaine (Sigma, St. Louis, USA) was prepared into a 1 M stock in ASW with a final stock of 1 mM in ASW and stored at 4°C.

Odonella sinensis cells (50-100μm long and 30-50μm wide) were plated onto in 30 mm Petri dish chamber into which poly-L-lysine coated glass coverslips had been cemented over a central aperture. Bath volume was 1ml and cells were perfused with ASW from a gravity fed reservoir prior to impalement (1.5 ml min^{-1}). For both the current and voltage clamp experiments, initial control recordings were conducted under ASW perfusion. The perfusion was then stopped and a 0.5 ml bolus addition of ASW (n = 7), 1 μM PbTx-3 (n = 14) or 1 ml bolus addition of 1 mM Lidocaine (n = 4) was added to the bath and the cells were incubated in the

medium for at least 15 before being washed with ASW by perfusion for an additional 15-30 min. All experiments were conducted under room temperature (20-22°C). To avoid artifacts due to possible osmotic changes over longer incubations under stopped flow, only 15 min time interval were analyzed.

Statistical Analysis

Numerical data are presented as the mean ± SE. Data for control and PbTx-3 treatments were analyzed using a paired Student's t-test (Systat, Chicago, USA) with an alpha level of ≤0.05 chosen to represent significant differences.

Figure 1. Brevetoxin binding site on voltage-gated sodium channels. Based on the amino acid residues of the PbTx-3 binding site found by Trainer et al. [16], from the multiple sequence alignment of eukaryote Na^+ VGCs using MEGA 4.0 [51] ,the binding site residues are labeled in yellow. Highly conserved residues of the transmembrane segments are highlighted in grey. Sequences were obtained from NCBI and JGI genome databases with acquisition numbers indicated.

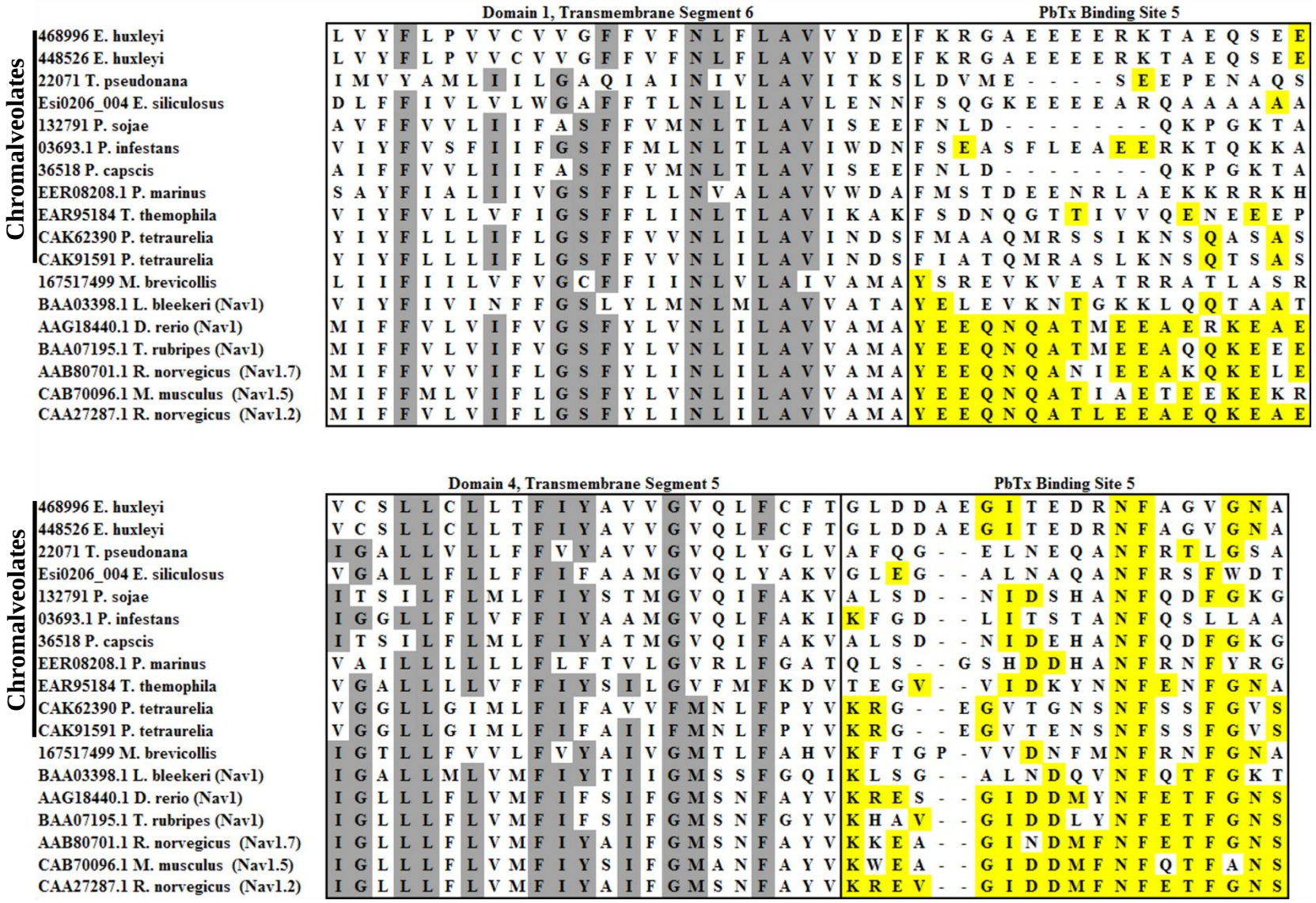

Chromalveolates
Domain 1, Transmembrane Segment 6
PbTx Binding Site 5
468996 E. huxleyi
448526 E. huxleyi
22071 T. pseudonana
Esi0206_004 E. siliculosus
132791 P. sojae
03693.1 P. infestans
36518 P. capscis
EER08208.1 P. marinus
EAR95184 T. themophila
CAK62390 P. tetraurelia
CAK91591 P. tetraurelia
167517499 M. brevicollis
BAA03398.1 L. bleekeri (Nav1)
AAG18440.1 D. rerio (Nav1)
BAA07195.1 T. rubripes (Nav1)
AAB80701.1 R. norvegicus (Nav1.7)
CAB70096.1 M. musculus (Nav1.5)
CAA27287.1 R. norvegicus (Nav1.2)
Chromalveolates
Domain 4, Transmembrane Segment 5
PbTx Binding Site 5
468996 E. huxleyi
448526 E. huxleyi
22071 T. pseudonana
Esi0206_004 E. siliculosus
132791 P. sojae
03693.1 P. infestans
36518 P. capscis
EER08208.1 P. marinus
EAR95184 T. themophila
CAK62390 P. tetraurelia
CAK91591 P. tetraurelia
167517499 M. brevicollis
BAA03398.1 L. bleekeri (Nav1)
AAG18440.1 D. rerio (Nav1)
BAA07195.1 T. rubripes (Nav1)
AAB80701.1 R. norvegicus (Nav1.7)
CAB70096.1 M. musculus (Nav1.5)
CAA27287.1 R. norvegicus (Nav1.2)

Figure 2. Uptake and cellular localization of Bodipy-PbTx-B in *Odontella sinensis.* Fluorescent confocal sectioning of *O. sinensis* treated with Bodipy-PbTx-B for 2 hrs (6 experiments, B, F, and J). Co-localization experiments of chlorophyll (6 experiments, C), mitochondria (1 experiment, G) and lipid bodies (1 experiment, K) were conducted, with only lipids showing accumulation of Bodipy-PbTx-B (L, arrowheads). In each micrograph N = nucleus.

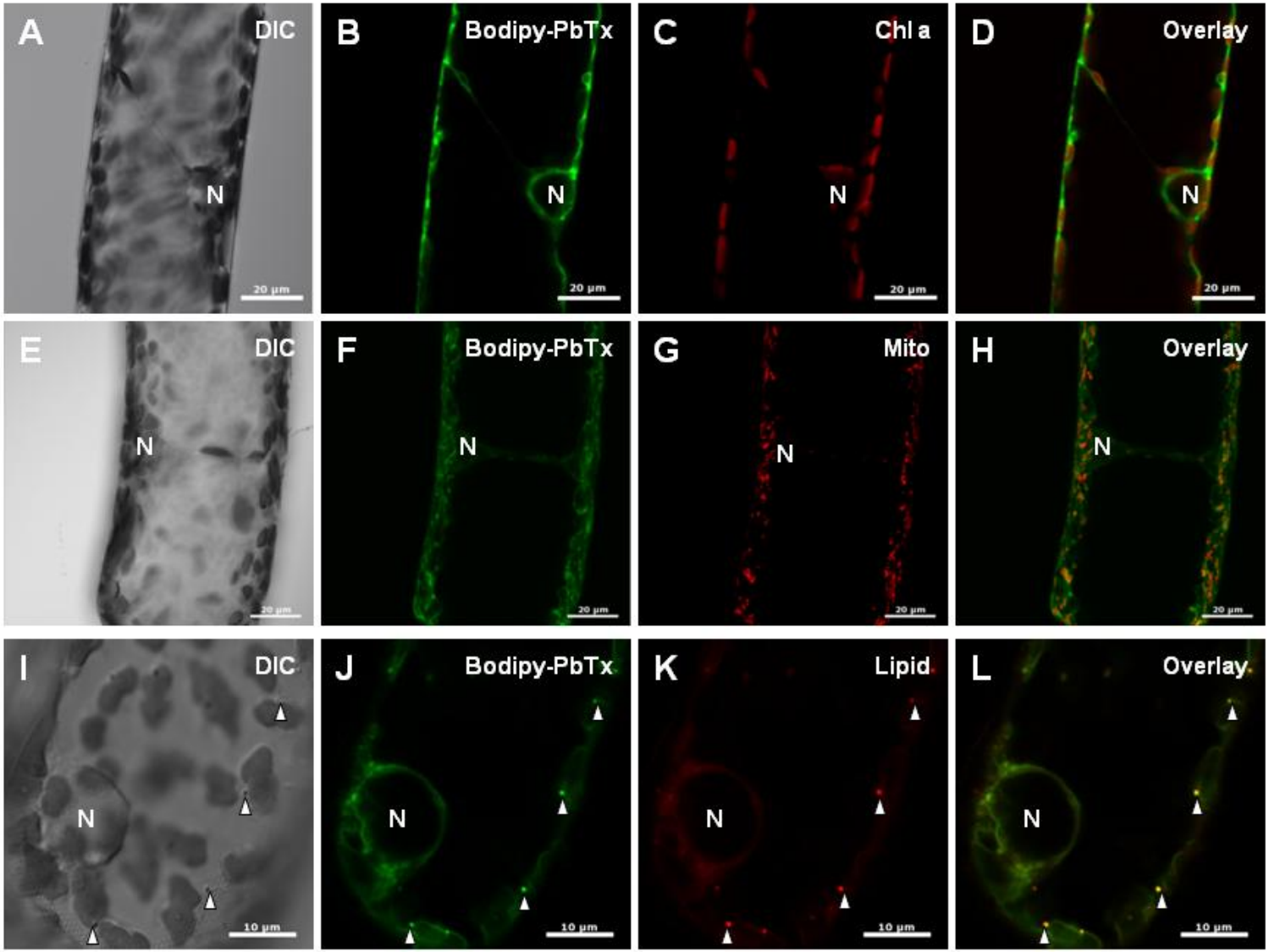

A
DIC
N
20 µm
B
Bodipy-PbTx
N
20 µm
C
Chl a
N
20 µm
D
Overlay
N
20 µm
E
DIC
N
20 µm
F
Bodipy-PbTx
N
20 µm
G
Mito
N
20 µm
H
Overlay
N
20 µm
I
DIC
N
10 µm
J
Bodipy-PbTx
N
10 µm
K
Lipid
N
10 µm
L
Overlay
N
10 µm

Figure 3. *K. brevis* is resistant to Bodipy-PbTx-B uptake. There was no detectable uptake of Bodipy-PbTx-B over a 4 hr incubation time (4 experiments, B, F, and J). Chlorophyll (C), mitochondria (G) and lipid bodies (K) were identified in *K. brevis* cells using autofluorescence and fluorescent probes. MitoTracker Orange CMTMRos and Nile Red.

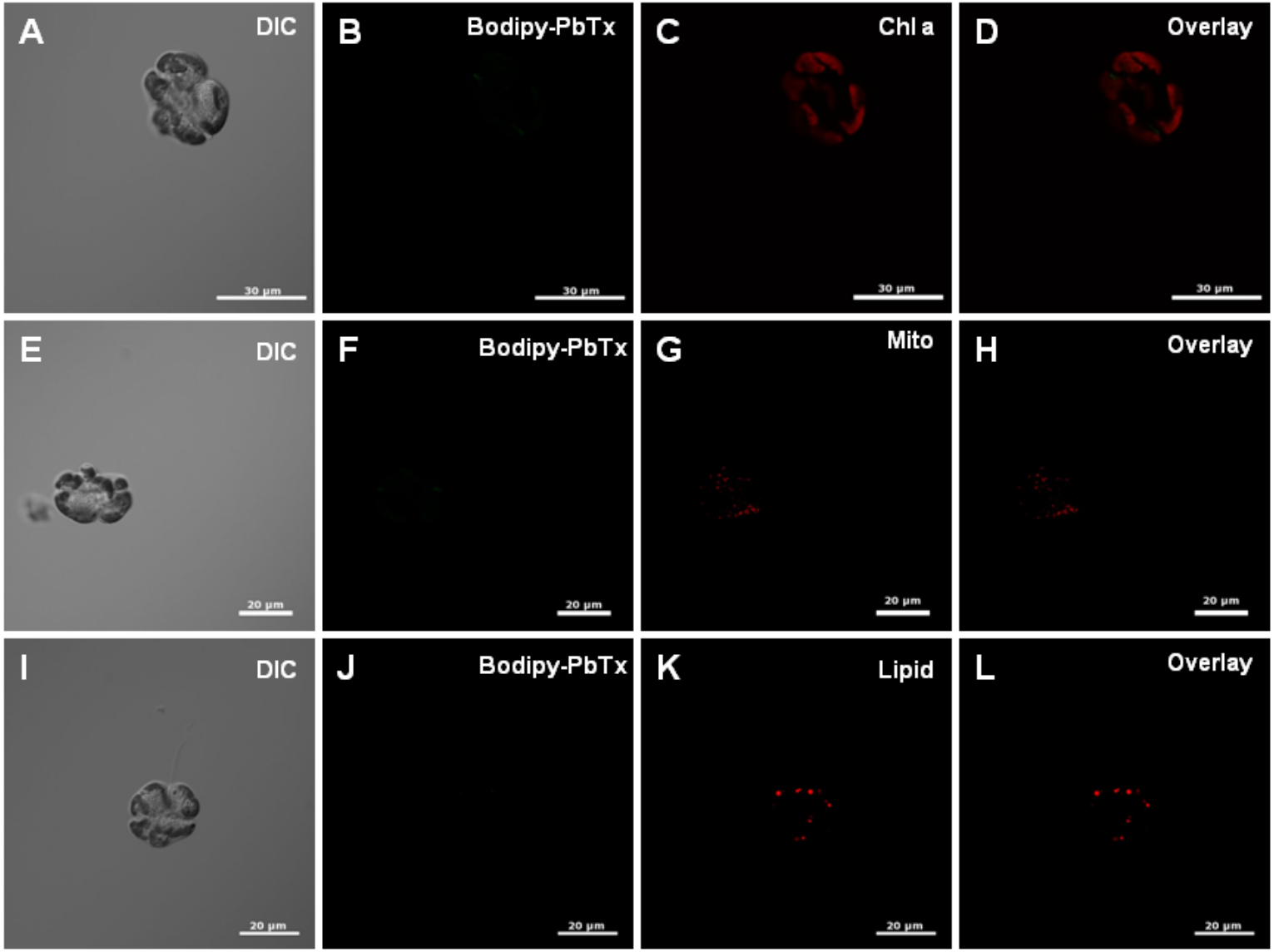

A
DIC
30 µm
B
Bodipy-PbTx
30 µm
C
Chl a
30 µm
D
Overlay
30 µm
E
DIC
20 µm
F
Bodipy-PbTx
20 µm
G
Mito
20 µm
H
Overlay
20 µm
I
DIC
20 µm
J
Bodipy-PbTx
20 µm
K
Lipid
20 µm
L
Overlay
20 µm

Figure 4. Spontaneous and evoked action potentials in *O. sinensis*. Two representative traces of a slower single action potential (A) and faster multiple spiking action potentials (B) observed while monitoring the resting membrane potential. The action potential can be evoked when injected with current (nA) for 10 ms (C) (n = 24).

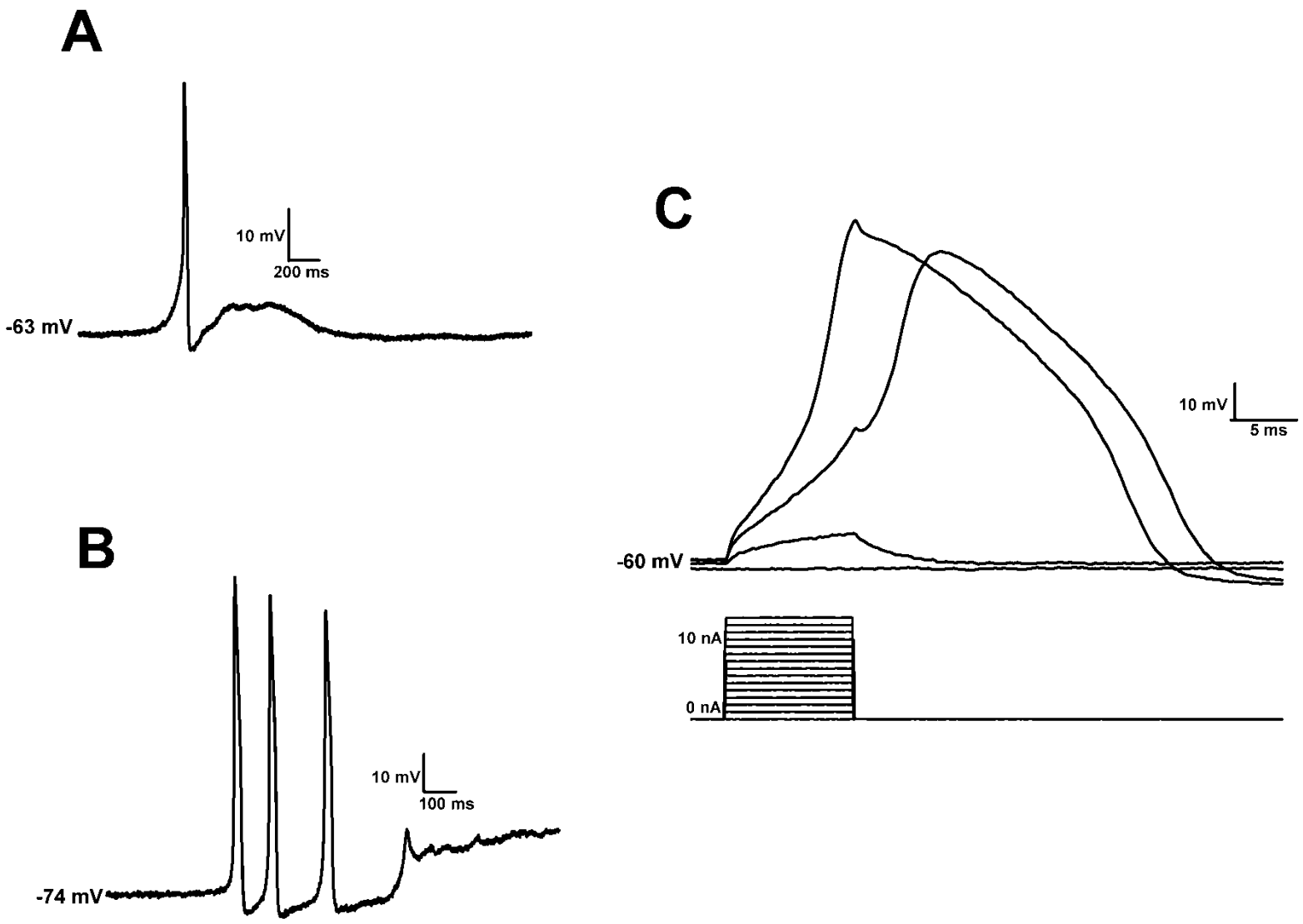

A
10 mV
200 ms
-63 mV
B
10 mV
100 ms
-74 mV
C
10 mV
5 ms
-60 mV
10 nA
0 nA

Figure 5. Effect of PbTx-3 on the *O. sinensis* membrane potential. Representative traces show free-running membrane potential monitored over 15 minutes following additions of ASW (A) and PbTx-3 (B and C) indicated by arrows.

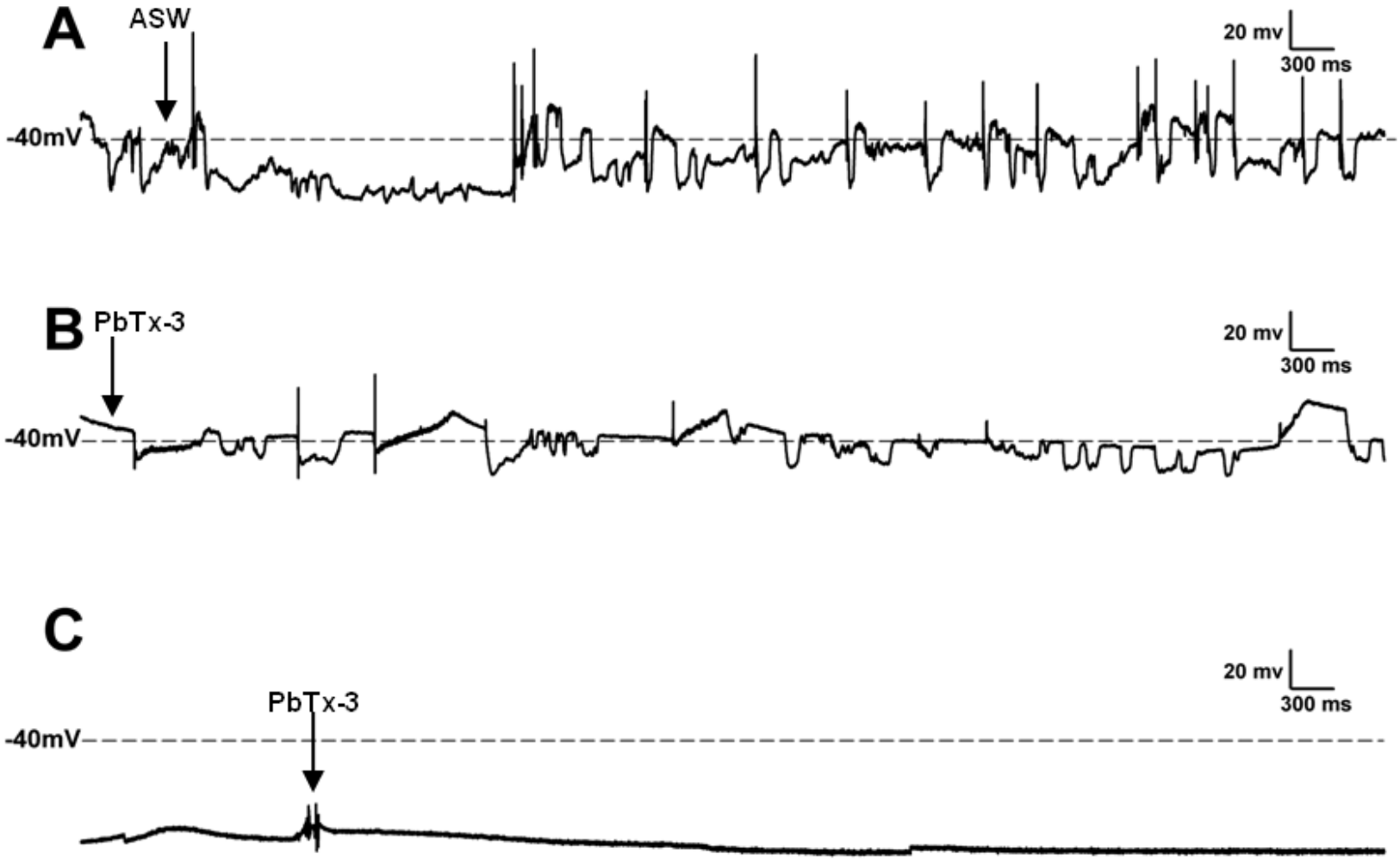

A
ASW
20 mv
300 ms
-40mV
B
PbTx-3
20 mv
300 ms
-40mV
C
20 mv
300 ms
PbTx-3
-40mV

Figure 6. Effects of PbTx-3 on *O. sinensis* voltage activated currents. In the control, a representative treatment of bolus ASW before (A) and after 15 minutes (B) with no change in inward current amplitude (n = 7). The dramatic decline in current amplitude after treatment with 1 µm PbTx-3 for 15 min (D) compared to the control (C) can easily be seen in the representative cell (n = 14). Inhibition of ion conductance at -60 mV by 1 µm PbTx-3 is illustrated in E. Average peak current were plotted as a function of membrane voltage for the inward current in the absence (○) and presence of 1 µm PbTx-3 (●), and for the outward current in the absence (△) and presence of 1 µm PbTx-3(▲). Standard error bars are indicated.

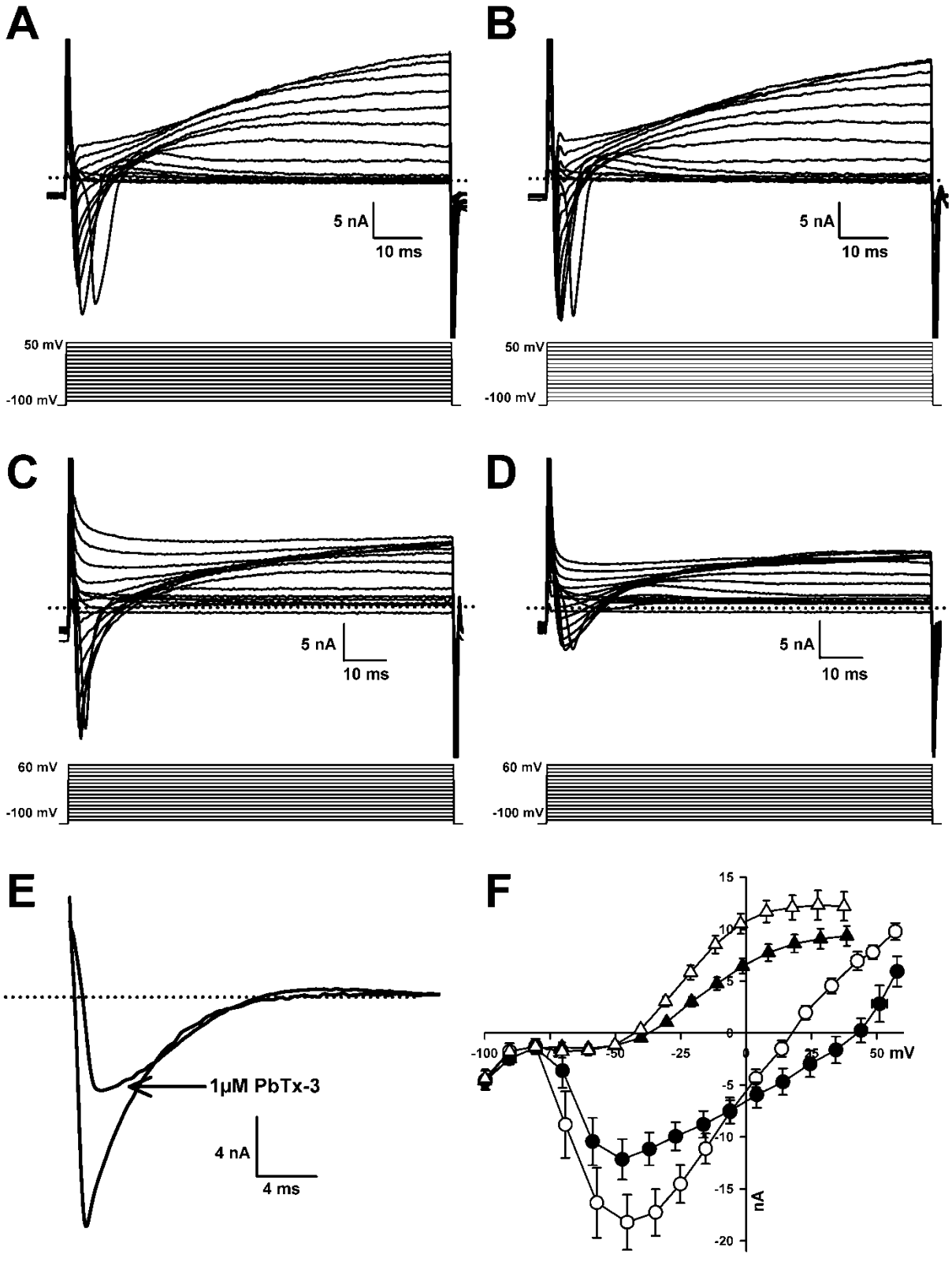

A
5 nA
10 ms
50 mV
-100 mV
B
5 nA
10 ms
50 mV
-100 mV
C
5 nA
10 ms
60 mV
-100 mV
D
5 nA
10 ms
60 mV
-100 mV
E
1μM PbTx-3
4 nA
4 ms
F
15
10
5
0
-5
-10
-15
-20
-100
-50
-25
50 mV
nA

Figure 7. Summary of lidocaine and PbTx inhibition of *O. sinensis* VGCs. Summary of the effects of lidocaine and PbTx-3 on the peak sodium current. Number of experiments and standard error bars are given for each treatment.

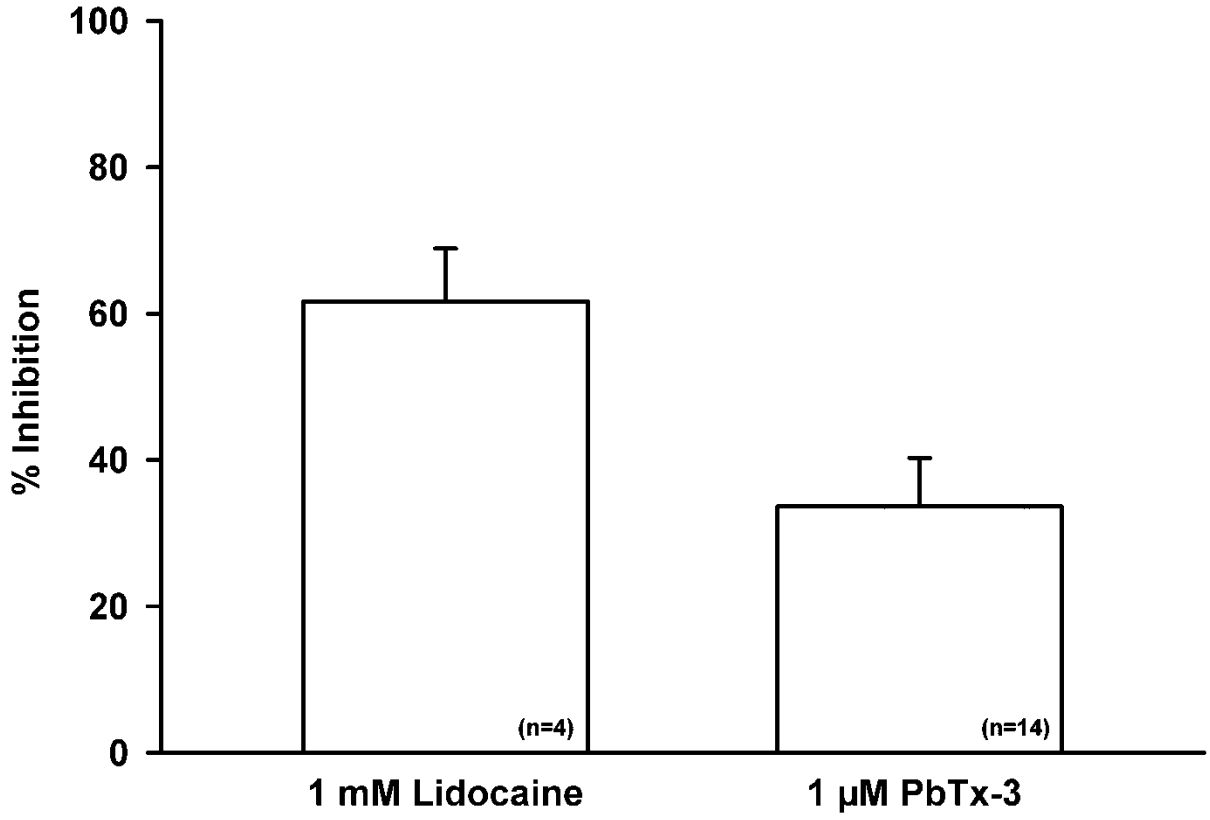

100
80
60
40
20
0
% Inhibition
(n=4)
(n=14)
1 mM Lidocaine
1 µM PbTx-3

Figure 8. Activation kinetics are unaffected by PbTx-3 addition. The average sodium conductance was measured for each voltage pulse and normalized to the maximum sodium conductance. The values were fitted to a Boltzmann distribution. There was little shift in the activation of the sodium current in the presence of 1μm PbTx-3 (●). Standard error bars are indicated.

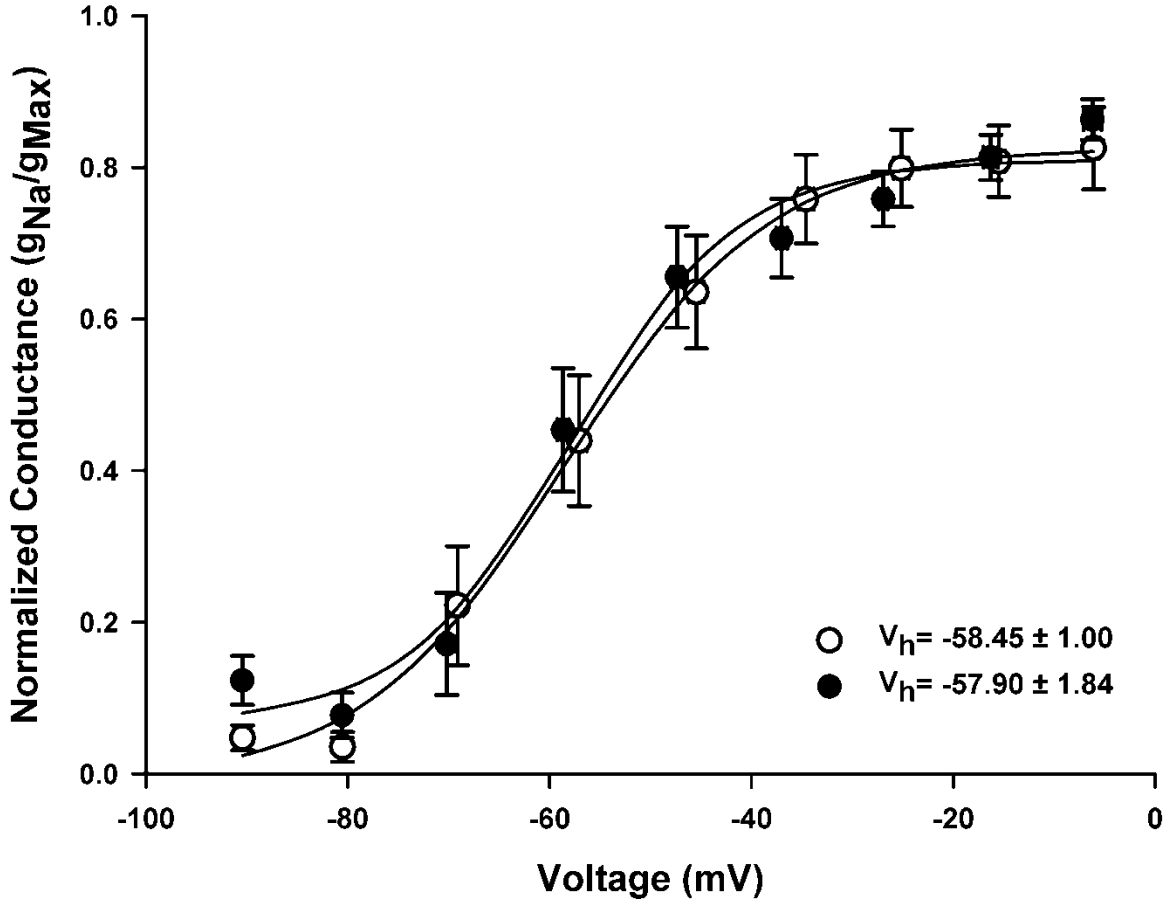

1.0
0.8
0.6
0.4
0.2
0.0
Normalized Conductance (gNa/gMax)
-100
-80
-60
-40
-20
0
Voltage (mV)
Vh= -58.45 ± 1.00
Vh= -57.90 ± 1.84

Figure 9. Inactivation kinetics of VGCs in *O. sinensis* in the presence of PbTx-3.
Representative traces are presented of the inactivation protocol in the control (A) and 1μm PbTx-3 treatments (B). The average values were normalized to the maximum peak current and fitted to a Boltzmann curve. There is a significant ($p < 0.05$) positive shift in the inactivation under PbTx-3 interaction (●, C). Standard error bars are shown.

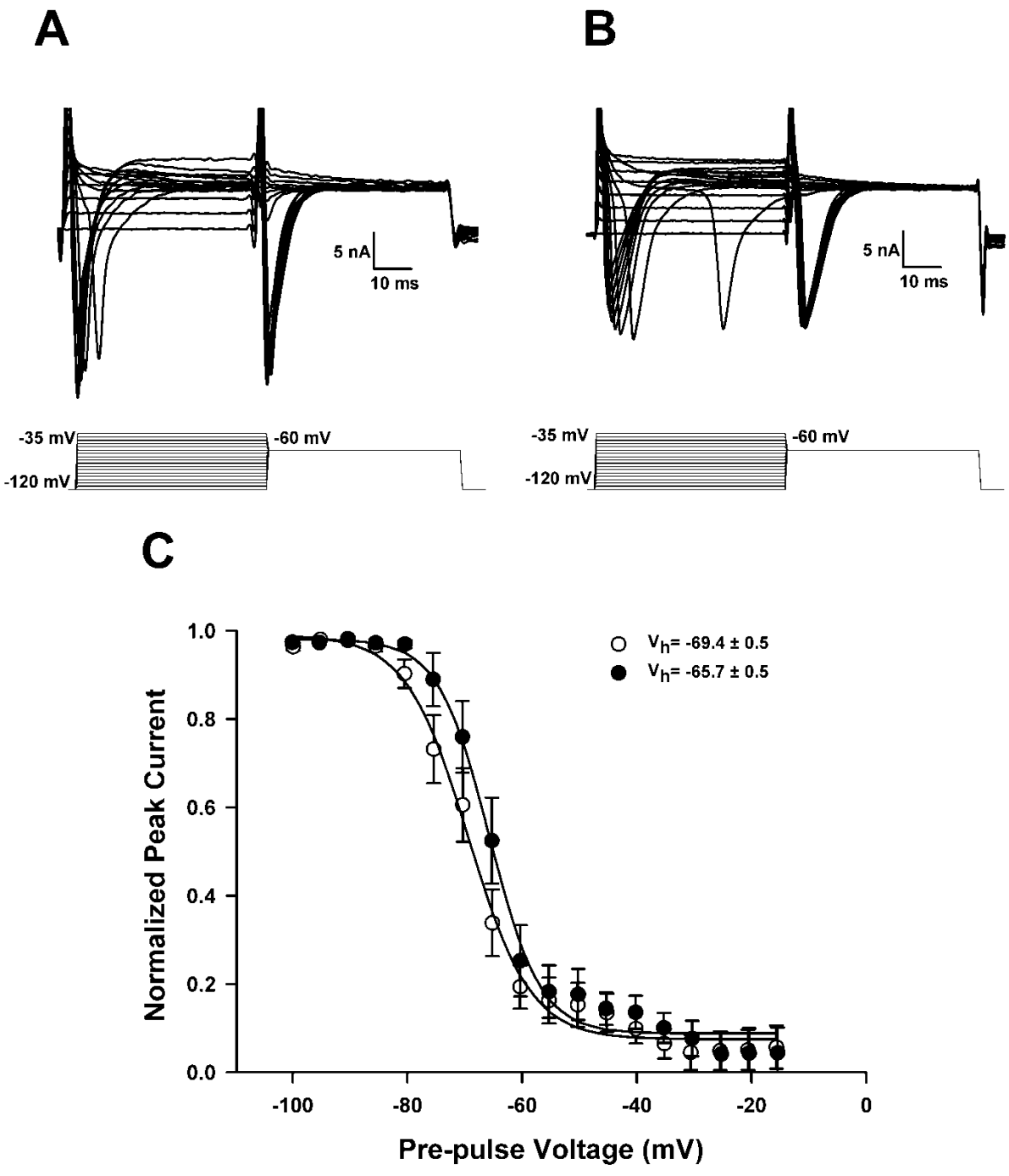
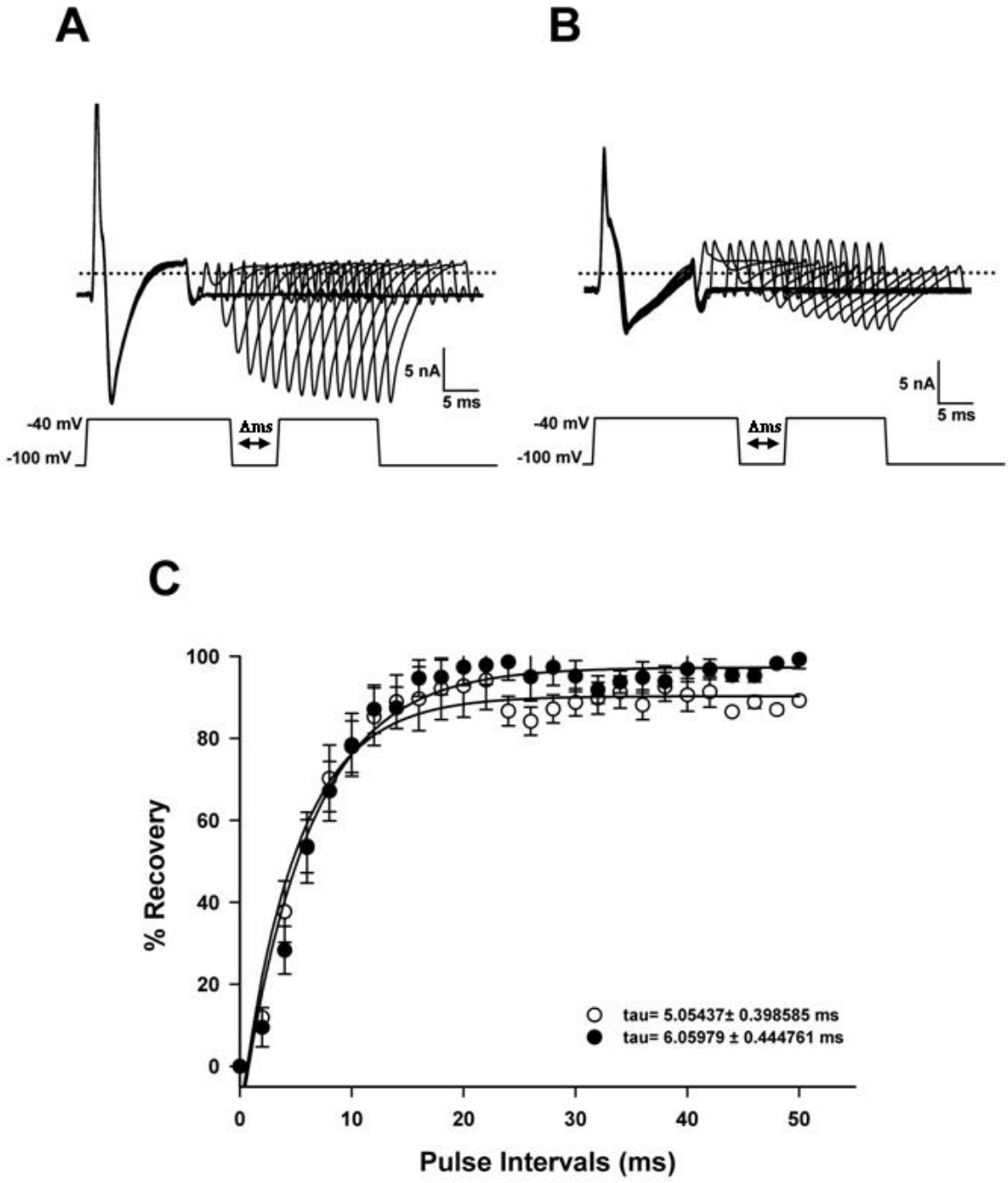

A
B
5 nA
10 ms
5 nA
10 ms
-35 mV
-120 mV
-60 mV
-35 mV
-120 mV
-60 mV
C
V_h= -69.4 ± 0.5
V_h= -65.7 ± 0.5
Normalized Peak Current
1.0
0.8
0.6
0.4
0.2
0.0
-100
-80
-60
-40
-20
0
Pre-pulse Voltage (mV)

Figure 10. The effects of PbTx-3 on the recovery from inactivation. A double pulse protocol was used, where the first depolarization pulse of voltage evoked a full sodium current followed by a short recovery time that increased each sweep by Δ ms. Then a second depolarization pulse of voltage was injected to evoke a current response following recovery time. The representative recovery from inactivation traces for the control (A) and 1 μM PbTx-3 treatments (B) show a similar pattern of recovery but a decrease in current amplitude in B. Capacity transients were removed from the current responses. The percent recovery graph (C) is a plot of the second evoked current following the voltage pre-pulse expressed as a percentage of the first peak current and is plotted against the time interval. There is little change in the control recovery time compared to the 1 μm PbTx-3 (●). Standard error bars are indicated.


A
B
5 nA
5 ms
-40 mV
-100 mV
Δms
C
% Recovery
Pulse Intervals (ms)
tau= 5.05437± 0.398585 ms
tau= 6.05979 ± 0.444761 ms

References

1. Cavalier-Smith T (2003) Genomic reduction and evolution of novel genetic membranes and protein-targeting machinery in eukaryote-eukaryote chimaeras (meta-algae). Philosophical Transactions of the Royal Society of London Series B: Biological Sciences 358: 109-134.
2. Armbrust EV, Berges JA, Bowler C, Green BR, Martinez D, et al. (2004) The genome of the diatom *Thalassiosira pseudonana*: Ecology, evolution, and metabolism. Science 306: 79-86.
3. Keeling PJ (2004) Diversity and evolutionary history of plastids and their hosts. American Journal of Botany 91: 1481-1493.
4. Moustafa A, Beszteri B, Maier UG, Bowler C, Valentin K, et al. (2009) Genomic footprints of a cryptic plastid endosymbiosis in diatoms. Science 324: 1724-1726.
5. Nosenko T, Bhattacharya D (2007) Horizontal gene transfer in chromalveolates. BMC Evolutionary Biology 7: 173.
6. Catterall WA (2000) From ionic currents to molecular mechanisms: The structure and function of voltage-gated sodium channels. Neuron 26: 13-25.
7. Taylor AR (2009) A Fast Na^{+}/Ca^{2+} Based Action Potential in a Marine Diatom. PLoS ONE 4: e4966.
8. Nejstgaard JC, Solberg PT (1996) Repression of copepod feeding and fecundity by the toxic haptophyte *Prymnesium patelliferum*. Sarsia 81: 339-344.
9. Miralto A, Barone G, Romano G, Poulet SA, Ianora A, et al. (1999) The insidious effect of diatoms on copepod reproduction. Nature 402: 173.
10. Kubanek J, Snell TW, Pirkle C (2007) Chemical defense of the red tide dinoflagellate *Karenia brevis* against rotifer grazing. Limnology and Oceanography 52: 1026-1035.
11. Fistarol GO, Legrand C, Graneli E (2003) Allelopathic effect of *Prymnesium parvum* on a natural plankton community. Marine Ecology-Progress Series 255: 115-125.
12. Teegarden GJ (1999) Copepod grazing selection and particle discrimination on the basis of PSP toxin content. Marine Ecology-Progress Series 181: 163-176.
13. Tillmann U, Alpermann T, John U, Cembella A (2008) Allelochemical interactions and short-term effects of the dinoflagellate *Alexandrium* on selected photoautotrophic and heterotrophic protists. Harmful Algae 7: 52-64.
14. Freeberg LA, Marshall A, Heyl M (1978) Interrelationships of *Gymnodinium breve* (Florida red tide) within the phytoplankton community. In: Taylor DL, Seliger HH, editors. Toxic Dinoflagellate Blooms. 1978 ed. New York: Elsevier. pp. 139-144.
15. Gawley RE, Rein KS, Kinoshita M, Baden DG (1992) Binding of brevetoxins and ciguatoxin to the voltage-senstive sodium-channel and conformational analysis of brevetoxin-B. Toxicon 30: 780-785.
16. Trainer VL, Baden DG, Catterall WA (1994) Identification of peptide components of the brevetoxin receptor site of rat brain sodium channels. Journal of Biological Chemistry 269: 19904-19909.
17. Baden D, Bourdelais AJ, Jacocks H, Michelliza S, J. N (2005) Natural and derivative brevetoxins: historical background, multiplicity, and effects. Environmental Health Perspectives 113: 621-625.

18. Baden DG (1989) Brevetoxins-unique polyether dinoflagellate toxins. FASEB Journal 3: 1807-1817.
19. Baden D, Rein K, Gawley R (1998) Marine toxins: how they are studied and what they can tell us. In: Cooksey KE, editor. Molecular Approaches to the Study of the Ocean. London: Chapman and Hall.
20. Huang JM, Wu CH, Baden DG (1984) Depolarizing action of a red-tide dinoflagellate brevetoxin on axonal membranes. The Journal of Pharmacology and Experimental Therapeutics 229: 615-621.
21. Ulbricht W (2005) Sodium channel inactivation: molecular determinants and modulation. Physiological Reviews 85: 1271-1301.
22. Sheridan RE, Adler M (1989) The actions of a red tide toxin form *Ptychodiscus brevis* on single sodium channels in mammalian neuroblastoma cells. FEBS Letters 247: 448-452.
23. Atchison WD, Luke VS, Narahashi T, Vogel SM (1986) Nerve membrane sodium chanenls as the target site of brevetoxins at neuromuscular junctions. British Journal of Pharamcology 89: 731-738.
24. Steidinger KA (2009) Historical perspective on *Karenia brevis* red tide research in the Gulf of Mexico. Harmful Algae 8: 549-561.
25. Vargo GA (2009) A brief summary of the physiology and ecology of *Karenia brevis* Davis (G. Hansen and Moestrup comb. nov.) red tides on the West Florida Shelf and of hypotheses posed for their initiation, growth, maintenance, and termination. Harmful Algae 8: 573-584.
26. Hallegraeff GM (1993) A review of harmful algal blooms and their apparent global increase. . Phycologia 32: 79-99.
27. Landsberg JH, Flewelling LJ, Naar J (2009) *Karenia brevis* red tides, brevetoxins in the food web, and impacts on natural resources: Decadal advancements. Harmful Algae 8: 598-607.
28. Breier CF, Buskey EJ (2007) Effects of the red tide dinoflagellate, *Karenia brevis*, on grazing and fecundity in the copepod *Acartia tonsa*. Journal of Plankton Research 29: 115-126.
29. Cohen JH, Tester PA, Forward RB, Jr. (2007) Sublethal effects of the toxic dinoflagellate *Karenia brevis* on marine copepod behavior. Journal of Plankton Research 29: 301-315.
30. Sotka EE, McCarty A, Monroe EA, Oakman N, Van Dolah FM (2009) Benthic herbivores are not deterred by brevetoxins produced by the red tide dinoflagellate *Karenia brevis* Journal of Chemical Ecology 35: 851-859.
31. Myers TL, Prince EK, Naar J, Kubanek J (2008) Loss of waterborne brevetoxins from exposure to phytoplankton competitors. Harmful Algae 7: 762-771.
32. Prince EK, Myers TL, Kubanek J (2008) Effects of harmful algal blooms on competitors: Allelopathic mechanisms of the red tide dinoflagellate *Karenia brevis*. Limnology and Oceanography 53: 531-541.
33. Prince EK, Myers TL, Naar J, Kubanek J (2008) Competing phytoplankton undermines allelopathy of a bloom-forming dinoflagellate. Proceedings of the Royal Society B: Biological Sciences 275: 2733-2741.
34. Jeglitsch G, Rein K, Baden DG, Adams DJ (1998) Brevetoxin-3 (PbTx-3) and its derivatives modulate single tetrodotoxin-sensitive sodium channels in rat sensory neurons. Journal of Pharmacology and Experimental Theraputics 284: 516-525.

35. Strachan LC, Lewis RJ, Nicholson GM (1999) Differential actions of pacific ciguatoxin-1 on sodium channel subtypes in mammalian sensory neurons. The Journal of Pharmacology and Experimental Therapeutics 288: 379-388.
36. Poli MA, Mende TJ, Baden DG (1986) Brevetoxins, unique activators of voltage-sensitive sodium channels, bind to specific sites in rat brain synatosomes. Molecular Pharmacology 30: 129-135.
37. Kim YS, Mandel LJ, Westerfield M, Padilla GM, Moore JW (1975) Effect of *Gymondinium breve* toxin(s) on frog skin and the giant axon of the squid. Environmental Letters 9: 255-264.
38. Westerfield M, Moore JW, Kim YS, Padilla M (1977) How *Gymnodinium breve* red tide toxin(s) produces repetitive firing in squid axons. American Journal of Physiology 232: C23-C29.
39. Bottein Dechraoui M-Y, Ramsdell JS (2003) Type B brevetoxins show tissue selectivity for voltage-gated sodium channels: comparison of brain, skeletal muscle and cardiac sodium channels. Toxicon 41: 919-927.
40. Bottein Dechraoui M-Y, Wacksman JJ, Ramsdell JS (2006) Species selective resistance of cardiac muscle voltage gated sodium channels: Characterization of brevetoxin and ciguatoxin binding sites in rats and fish. Toxicon 48: 702-712.
41. Moffat MC (1994) An ultrastructural study of *Didymosphenia geminata* (Bacillariophyceae). Transactions of the American Microscopy Society 113: 59-71.
42. Drum RWaP, H.S. (1964) Pyrenoids, raphes and other fine structures in diatoms. American Journal of Botany 51: 405-418.
43. Kubanek J, Hicks MK, Naar J, Villareal TA (2005) Does the red tide dinoflagellate *Karenia brevis* use allelopathy to outcompete other phytoplankton? Limnology and Oceanography 50: 883-895.
44. Vardi A, Formiggini F, Casotti R, De Martino A, Ribalet F, et al. (2006) A stress surveillance system based on calcium and nitric oxide in marine diatoms. PloS Biology 4: 411-419.
45. Falciatore A, d'Alcala MR, Croot P, Bowler C (2000) Perception of environmental signals by a marine diatom. Science 288: 2363-2366.
46. Guillard RRL, Ryther JH (1962) Studies of marine planktonic diatoms I. *Cyclotella nana* Hustedt and *Detonula confervacea* Cleve. . Canadian Journal of Microbiology 8: 229-239.
47. Guillard RRLaH, P.E. (1993) *Stichochrysis immobilis* is a diatom, not a chrysophyte. Phycologia 32: 234-236.
48. Loeblich AR (1975) A seawater medium for dinoflagellates and the nutrition of *C. niei*. Journal of Phycology 11: 80-86.
49. Altschul SF, Gish W, Miller W, Myers EW, Lipman DJ (1990) Basic local alignment search tool. Journal of Molecular Biology 215: 403-410.
50. Thompson JD, Higgins DG, Gibson TJ (1994) CLUSTAL W: improving the sensitivity of progressive multiple sequence alignment through sequence weighting, position-specific gap penalties and weight matrix choice. Nucleic Acids Research 22: 4673-4680.
51. Tamura K, Dudley J, Nei M, Kumar S (2007) MEGA4: Molecular Evolutionary Genetics Analysis (MEGA) software version 4.0. Molecular Biology and Evolution 24: 1596-1599.

52. Lam CMC, Yeung PKK, Wong JTY (2005) Monitoring cytosolic calcium in the dinoflagellate *Crypthecodinium cohnii* with calcium orange-AM. Plant Cell Physiology 46: 1021-1027.